Energy Gains and Losses in Be Star Envelopes

by

Carol Evelyn Millar

Department of Physics and Astronomy

Graduate Program in Astronomy

Submitted in partial fulfilment

of the requirements for the degree of

Doctor of Philosophy

Faculty of Graduate Studies

The University of Western Ontario

London, Ontario

January 2000

Abstract

I have successfully developed a method to determine the kinetic temperature of the electron gas as a function of position in the circumstellar envelopes of Be stars independent of the model for the density distribution of the gas. My method yields a self-consistent solution of the equation for energy conservation, thus eliminating the necessity to assume arbitrarily a temperature for the gas. This technique has been applied to Be stars of differing effective temperatures using several models.

The shape and relative line strength of the observed Hα line for several Be stars was matched successfully for some models with the temperatures determined self-consistently. The density, which must be assumed at one position in the envelope, was varied until the relative strength of the line matched observations. This procedure provides a useful method to test and adjust the assumed density.

In order to approximate better the physical conditions in the envelope, I have also investigated the role of the diffuse radiation field in the Lyman continuum, which is produced within the envelope, using the on-the-spot approximation. This approximation allows an upper limit to the temperature to be determined. Generally, the diffuse radiation increases the degree ionization which leads to increased heating. The effect of the diffuse radiation is particularly important for very dense envelopes and/or for late-type Be stars which have fewer ionizing photons.

It has been argued by some researchers that the re-processing efficiency of the envelope is not great enough to produce the observed flux without an additional source of ionizing radiation. To test this, the total integrated flux produced by various lines was predicted and compared with observations for a range of Be stars. My models, which assume the central star is the only source of ionizing radiation, produce total fluxes in Hα, Pα, and Brα which account for the observed emission.

Keywords: Astronomy, stellar physics, early-type stars, circumstellar matter, emission-line stars, Be stars.

This thesis is dedicated to my sons, Mark and David,

to my parents, Don and Evelyn Theaker,

and to my best friend, James Delmar Jones,

in thanks for continued interest and support.

Co-Authorship

This thesis contains material from previously published manuscripts and manuscripts accepted for publication, co-authored by: J. M. Marlborough and T. A. A. Sigut. For copyright releases, declarations of co-author consent and detailed descriptions of co-author contributions, see Appendices A and B. Herein I describe my personal contribution to individual chapters:

- **Chapter 2. Self-Consistent Temperature Distribution for γ Cas**

  I modified an existing code to calculate the rates of energy gain and loss due to photoionization, radiative recombination, collisional processes, and free-free emission and absorption in the envelope, performed necessary computations and wrote the manuscript.

- **Chapter 3. 1 Delphini**

  I modified an existing line shape program to accommodate a variable temperature grid. I performed the necessary calculations and wrote the manuscript.

- **Chapter 4. Diffuse Radiation**

  The necessary changes to the existing program were made in order to approximate the effect of diffuse radiation produced within the envelope. I performed the necessary calculations and wrote the manuscript.

- **Chapter 5. The Disk Model**

  I modified the disk model code to compute the rates of energy gain and loss. Then I performed the necessary calculations and wrote the manuscript.

- **Chapter 6. Energetics of Be Star Envelopes**

  Various models which I developed for several Be star envelopes were computed. The output from these models was used to integrate the total flux in various lines to

compare to observations. The integration program was written by T. A. A. Sigut. I wrote the manuscript.

Acknowledgement

A special thanks to my advisor Mike Marlborough. The time spent at Western working with Mike has been most enjoyable.

Thanks to members of the Physics and Astronomy Department and especially to members of the Astronomy Group for helping to make the time I spent at Western during both my undergraduate and graduate programs both memorable and successful. Special thanks and best wishes to my fellow Astronomy graduate students/postdocs: Todd Fuller, Steve Shorlin, Aaron Sigut, Rob Thacker, Eric Tittley and Gregg Wade.

Financial support provided by NSERC, the Natural Sciences and Engineering Research Council of Canada, for four years of graduate study (in the form of PGS A and PGS B postgraduate scholarships) is greatly appreciated and contributed to the completion of this work.

This manuscript was prepared using a version UWO Thesis and Project LaTeX style, originally developed by Khun Yee Fung and modified by Eric Tittley.

Table of Contents

List of Tables

List of Figures

List of Appendices

Chapter 1

Introduction

1.1 Be Stars

In 1866 Vatican astronomer Angelo Secchi identified Hβ emission in the star γ Cas (Secchi 1867). This detection marked the first observation of the class of stars now known as Be stars. B-emission (Be) stars are massive stars that show, or have shown in their spectra, Balmer emission lines originating from circumstellar gas. The radiation from the central star ionizes the surrounding gas, and the subsequent recombination of electrons produces the observed emission lines. The standard properties of Be stars include rapid rotation, non-radial pulsations, intrinsic linear polarization by electron scattering, infrared and radio excess due to free-free emission, UV absorption lines of high ionization species, and variability on a variety of time scales. Be stars also have winds which are composed of both a fast, hot, lower density polar wind and a slowly expanding, cool, higher density equatorial wind. Typically the density in the equatorial gas is a factor of 100 or so larger than the polar wind. This asymmetry in the envelope is directly revealed by the large degree of continuum linear polarization ($\sim 2\%$). Direct imaging has confirmed this view of a Be star (Dougherty and Taylor 1992, Quirrenbach et al. 1997, and Wood et al. 1997). One finds evidence for the Be phenomenon extending from O7 to early A stars (Slettebak 1991). In addition, there are some A stars which show evidence for circumstellar material, but do not exhibit Balmer emission lines (Marlborough 2000). Be stars are believed to be main sequence or slightly evolved stars (Slettebak 1988).

B stars have approximate masses and radii in the ranges, 3 to 15 $M_\odot$ and 3 to 7 $R_\odot$, respectively (Slettebak 1986). The luminosity range is approximately $2 \lesssim \log L/L_\odot \lesssim 4$ and

the effective temperature varies from 10000 K to 30000 K (Underhill and Doazan 1982). Be stars, for which the envelope becomes optically thin, exhibit spectra similar to normal B stars. The typical values for the rotational velocities, inferred from analysis of line profiles, are of the order of 100's of $\mathrm{km\,s^{-1}}$ (Slettebak 1986).

The mechanism by which the disks surrounding Be stars are formed and maintained is not known. Certainly, rapid rotation is an important prerequisite for the formation of the disk; however, since these stars are thought to rotate less than the critical velocity, at least one additional mechanism must be operating. (The critical velocity is the velocity at the stellar equator for which centrifugal force balances gravity.) There are many other mechanisms which have been proposed for the formation of these disks such as, non-radial pulsations (Vogt and Penrod 1983), non-spherical, radiatively-driven wind effects (Puls, Petrenz, and Owocki 1999), the wind compressed disk model (Bjorkman and Cassinelli 1993), bi-stable radiation-driven winds (Lamers and Pauldrach 1991), and interacting binary systems, but none of these has been completely successful.

A particular subclass of the Be stars is known as shell stars. These stars are characterized by hydrogen lines with wide emission wings together with narrow absorption cores and narrow absorption lines of ionized metals (Slettebak 1988). All shell stars are Be stars, but the reverse is not true. Some Be stars never exhibit spectral lines with the features which characterize shell stars. Some shell stars can be quite variable; the shell phase has been observed to come and go in some stars, for example, Pleione. In contrast, 1 Del has been observed to be quite stable and has not exhibited any long-term spectral variations (Marlborough and Cowley 1974).

A variety of other types of stars populate the upper main sequence. These include: O, Of and Oe stars, OB supergiants, B[e] stars, Herbig Ae/Be stars, and LBVs (luminous blue variables). The O, Of, Oe stars and OB supergiants are very luminous and are distinguished by high mass loss rates from stellar winds driven by radiation pressure. O stars are characterized by the presence of ionized He lines. Other spectral lines often observed include:

Si IV, C III, and N III which is only observed in emission (Jaschek and Jaschek 1987). If the star shows emission in the Balmer series, it is classified as Oe. If emission in N III *and* He II are present the star is classified as Of (Jaschek and Jaschek 1987). OB supergiants have H, He I, and He II spectral lines and have temperatures up to 50000 K. Mass loss rates range approximately from 10^{-7} to $10^{-6} M_\odot$ (Humphreys 1991). The B[e] stars share some similarities with Be stars such as Balmer emission lines and intrinsic linear polarization. However, B[e] stars are characterized by IR dust emission and forbidden emission lines usually Fe II and O I (Zickgraf 1988). Herbig Ae/Be stars are pre-main sequence objects of spectral type A or earlier with emission lines present. These objects are often obscured by nebulosity which is illuminated by the star (Zickgraf 1988). LBV stars are luminous, unstable hot supergiant stars. They are characterized by irregular eruptions which greatly increase their mass loss (10^{-5} to $10^{-4} M_\odot$) (Humphreys 1991). This outflow produces a dense, cool (8000 to 9000 K) envelope, and during these phases the star resembles a luminous A-type supergiant. During the quiescent stage, the much hotter photosphere (20000 to 25000 K) is evident, and the star resembles an OB supergiant (Humphreys 1991).

The Be stars represent a significant fraction of hot stars ($\sim 20\%$ of B stars are Be), and it is therefore important to understand the processes by which these disks are formed and maintained.

1.2 Theoretical Models

The general problem is to determine the density, velocity, and temperature in the circumstellar envelopes of Be stars as a function of both position and time. Models to describe the physical conditions in these disk-like winds can in principle be obtained from solutions of equations which express the conservation of mass, momentum, and energy, supplemented by the solution of the statistical equilibrium equations which describe the microscopic processes that gas particles undergo. If magnetic fields are present, then Maxwell's equations must be solved simultaneously with those listed above. It is not clear whether viscous forces are important. There may be other non-

radiative energy sources which need to be included in the energy gains and losses. These equations are, therefore, a complex set of non-linear partial differential equations. It is not possible to solve this complex set of equations exactly. To obtain solutions many simplifying assumptions must be made. Usually a steady state is assumed and gravitation, pressure gradients, and centrifugal forces are included but other non-radiative forces are omitted. Since magnetic fields have not been detected in any classical Be stars, these are usually omitted also.

The Poeckert-Marlborough model, (PM), developed originally by Marlborough (1969), and later modified by Poeckert and Marlborough (1978), successfully predicted and reproduced satisfactorily a large number of observable features in Be star spectra. I have developed a technique for determining self-consistent temperature for Be star envelopes. The PM model is the basis for much of the analysis in this thesis so I will now provide an outline of the basic details of this model.

The central star is assumed to be spherically symmetric and rotating at the critical velocity. The continuum energy distribution is given by Kurucz, Peytremann, and Avrett (1974). The envelope is assumed to be symmetric about both the rotation axis and the equatorial plane and is composed of pure hydrogen with 5 bound levels and the continuum. A density, $\rho_{\circ}$, must be assumed at a position in the equatorial plane. A velocity distribution is adopted; then the equation of mass conservation gives the density distribution in the equatorial plane. For example, γ Cas is assumed to have outflow velocities of 7.5, 8.0, 25.0, 125, and 200 km s^{-1} at radial distances from the central star of 1, 2, 6, 18, and 40 stellar radii, respectively. At a specified location in the equatorial plane, ω', the density distribution perpendicular to the equatorial plane is assumed to be hydrostatic; this sets the position and shape of the projection of the density streamlines in a meridional plane. As the value of this parameter increases, the emitting volume of the envelope also increases.

At each location within the envelope the energy density of radiation is determined assuming the star is the only source of energy input. The stellar surface was divided into 13

sectors, and the optical depth from predetermined locations within the envelope to each of these sectors was determined using an iterative Simpson routine. Only bound-free processes were included in these calculations. The continuum energy originating from the star was reduced, both geometrically and physically based on the optical depth to the star. Each recombination to the ground state in the envelope produces a photon which can ionize another atom. This diffuse radiation was not included in the PM model.

At predetermined locations within the envelope the level populations are obtained from a solution of the statistical equilibrium equations, assuming a steady state. The effect of the line radiation on the level populations is included in an approximate manner. The optical depth from each position in the envelope to the upper edge of the disk along a path perpendicular to the equatorial plane was calculated. Based on this value, 2 of 5 cases were considered: optically thin in all lines, optically thick in Lyman lines and thin in everything else, optically thick in Lyman and Balmer lines and thin in everything else, optically thick in Lyman, Balmer, and Paschen lines and thin in everything else, and optically thick in all lines. The final populations were a weighted mean of 2 cases. For addition details regarding the PM model, see Poeckert and Marlborough (1978) and Marlborough (1969).

The PM model was based on a number of simplifying assumptions. In particular, the equation for the conservation of energy was by-passed by assuming a simple functional form for the kinetic temperature of the circumstellar matter. For example, for γ Cas an isothermal envelope temperature of 20000 K was assumed. Such an ad hoc treatment of the disk temperature greatly limits a model's use as a diagnostic for the physical conditions in circumstellar winds by unnecessarily treating the disk temperature as yet another adjustable parameter.

Over the past few years, some astronomers, K. M. V. Apparao and the late S. P. Tarafdar for example, have questioned the choice of the assumed temperature in the circumstellar envelope. Apparao and Tarafdar (1987) claimed that there are not enough Lyman continuum

photons emitted from the star to ionize the gas and heat the envelope to the temperature assumed, and they postulate an additional source of envelope heating.

1.3 Self-Consistent Envelope Temperatures

My PhD thesis research project has been to develop techniques for determining the temperature structure of 2 dimensional models that describe the disk-like winds surrounding Be stars. No one previously has calculated the temperature in Be circumstellar disks in a self-consistent manner. I have developed a method for determining this temperature self-consistently throughout the circumstellar gas. An initial envelope temperature is assumed and the level populations are calculated. Based on these level populations the rates of energy gain and loss are determined throughout the envelope. My procedure enforces the conservation of energy by adjusting the temperature iteratively until the radiative energy gains and losses are equal throughout the envelope. Convergence to a unique value of temperature at all positions in the envelope was verified by choosing a variety of initial guesses for the temperature and ensuring, each time, that the final temperatures for a particular model were the same. I have applied this method to both the PM model and the disk model (Waters 1986). The improved models have been used to reinterpret the observed emission spectra of several Be stars, most notably γ Cas and 1 Del. As a result of my work, we now have a more consistent picture of the conditions in their disks (Millar and Marlborough 1998, 1999a, 1999b, and 1999c).

An additional complexity in calculating the energy balance in the circumstellar wind is to include the radiation field produced within the circumstellar gas itself. This radiation is commonly called the diffuse radiation field, and in addition to the direct radiation field from the central star, provides an additional source of heating. I have included the diffuse field by the on-the-spot approximation and demonstrated that it is critical in determining the correct thermal structure and ionization balance within the wind.

My method for determining the temperature not only provides a self-consistent temperature structure but also can be used to test the temperatures assumed for other Be stars by other researchers. The detailed models I have developed are an essential step to determine the physical parameters of stellar winds, to discover how these regions are formed and maintained, and to interpret observations.

1.4 Temperature as a Diagnostic Tool

The temperature directly determines the degree of ionization and hence the strength of spectral lines. Once the temperature is determined self-consistently, the values of other free parameters can be estimated with greater certainty. For example, the value of ρ_0, the density at a particular position in the equatorial plane which must be assumed before the equation of continuity is solved, can be adjusted until the observed and predicted lines match. If one includes chemical elements in addition to hydrogen in the model, then one can predict the location of the various ionization stages in the envelope. The broadening of lines of differing ionization stages allows the rotational velocity of the envelope as a function of distance from the star to be better constrained. At the present time, a simple velocity distribution as a function of distance from the star is usually assumed. Improved knowledge about the physical conditions and parameters of Be star envelope will allow various models which describe how these disks form and are maintained to be tested with greater certainty.

Bibliography

Apparao, K. M. V. & Tarafdar, S. P., 1987. *ApJ* **322**, 976.

Bjorkman, J. E. & Cassinelli, J. P., 1993. *ApJ* **409**, 429.

Dougherty, S. M. & Taylor, A. R., 1992. *Nature* **359**, 808.

Humphreys, R. M., 1991. Stars, high luminosity. In S. P. Maran (Ed.), *The Astronomy and Astrophysics Encyclopedia*, New York, Van Nostrand Reinhold.

Jaschek, C. & Jaschek, M., 1987. *The Classification of Stars*. Cambridge: Cambridge University Press.

Kurucz, R. L., Peytremann, E., & Avrett, E. H., 1974. *Blanketed model atmospheres for early-type stars*. U.S.A.: Washington : Smithsonian Institution.

Lamers, H. J. G. L. M. & Pauldrach, A. W. A., 1991. *A&A* **244**, L5.

Marlborough, J. M., 1969. *ApJ* **156**, 135.

Marlborough, J. M., 2000. Summary and future directions. In M. A. Smith, H. F. Henrichs, and J. Fabregat (Eds.), *IAU Colloq. 175, The Be Phenomenon in Early-Type Stars*.

Marlborough, J. M. & Cowley, A. P., 1974. *ApJ* **187**, 99. (MC).

Millar, C. E. & Marlborough, J. M., 1998. *ApJ* **494**, 715. (MM).

Millar, C. E. & Marlborough, J. M., 1999a. *ApJ* **516**, 280. (MMa).

Millar, C. E. & Marlborough, J. M., 1999b. *ApJ* **516**, 276. (MMb).

Millar, C. E. & Marlborough, J. M., 1999c. *ApJ* **526**, 400.

Poeckert, R. & Marlborough, J. M., 1978. *ApJ* **220**, 940. (PM).

Puls, J., Petrenz, P., & Owocki, S. P., 1999. In B. Wolf and A. W. Fullerton (Eds.), *IAU Colloq. 169, Variable and Non-spherical Stellar Winds in Luminous Hot Stars*, Germany. Springer-Verlag.

Quirrenbach, A., Bjorkman, K. S., Bjorkman, J. E., Hummel, C. A., Buscher, D. F., Armstrong, J. T., Mozurkewich, D., II, N. M. E., & Babler, B. L., 1997. *ApJ* **479**, 477.

Secchi, A., 1867. *Astron. Nachr.* **68**, 63.

Slettebak, A., 1986. *PASP* **98**, 867.

Slettebak, A., 1988. *PASP* **100**, 770.

Slettebak, A., 1991. Stars, Be-type. In S. P. Maran (Ed.), *The Astronomy and Astrophysics Encyclopedia*, New York. Van Nostrand Reinhold.

Underhill, A. B. & Doazan, V., 1982. *B Stars With and Without Emission Lines*, U.S.A.: NASA SP-465.

Vogt, S. S. & Penrod, G. D., 1983. *ApJ* **275**, 661.

Waters, L. B. F. M., 1986. *A&A* **162**, 121.

Wood, K., Bjorkman, K. S., & Bjorkman, J. E., 1997. *ApJ* **477**, 926.

Zickgraf, F. J., 1988. Current definition of B[e] stars. In A. M. Hubert and C. Jaschek (Eds.), *B[e] Stars*, Dordrecht. Kluwer Academic Publishers.

Chapter 2

Self-Consistent Temperature Distribution for γ Cas[1]

2.1 Introduction

We have determined the kinetic temperature of the electron gas as a function of position in the circumstellar envelopes of early Be stars for the model developed by Poeckert and Marlborough (1978), hereafter PM. The rates of energy gain and loss due to photoionization, radiative recombination, collisional transitions between bound levels, free-free emission, and free-free absorption were calculated at a set of grid points in a meridional plane. If the temperature assumed were correct, the ratio of energy gain to energy loss would be exactly unity at all points in the envelope. Our investigation demonstrates that the choice of a constant temperature of 20,000 K by PM, was a reasonable first order approximation. More importantly, we have also determined the temperature which corresponds to equal rates of energy gain and loss at each grid point throughout the envelope. These temperatures represent locally a self consistent solution of the equation of energy conservation.

Be stars exhibit hydrogen emission lines at optical and infrared wavelengths and frequently emission from singly ionized metals as well. The hydrogen emission lines arise by recombination in ionized circumstellar material, and are frequently variable on a wide range of time scales (Underhill and Doazan 1982). Further discussion of the emission lines and

[1] A version of this chapter has been published: Millar C. E., Marlborough J. M., (1998) Rates of energy gain and loss in the circumstellar envelopes of Be stars: the Poeckert-Marlborough model, ApJ, 494, 715.

the spectra of Be stars in other wavelength regions can be found in review articles in Balona et al. (1994), Slettebak and Snow (1987), and references therein.

It has long been accepted that the circumstellar emitting region of Be stars is not spherically symmetric (Coyne and McLean 1982). This expectation has been confirmed recently by direct imaging: Dougherty and Taylor (1992), Quirrenbach et al. (1993), and Stee et al. (1995); the circumstellar region is much more disk-like than spherical. In addition, recent results of Quirrenbach et al. (1997) and Wood et al. (1997) indicate that the disks around some Be stars are quite thin: for example, Wood et al. (1997) find a disk half-opening angle of 2.5 for ζ Tauri.

A complete hydrodynamical treatment of the structure and dynamics of this disk-like, circumstellar envelope is an overwhelmingly complex problem. Because of the complexity of the equations, initial models were more or less ad hoc (Marlborough 1976, 1987). More recently these ad hoc models have received some theoretical support. Bjorkman and Cassinelli (1993) have shown that, under certain restrictive assumptions, a radiation driven wind from the polar regions of a rapidly rotating star is deflected toward the equatorial plane. The part of the radiation driven wind near the equatorial plane is compressed, and this compressed, less rapidly expanding wind resembles qualitatively these ad hoc models. Owocki et al. (1994) confirmed this general picture by numerical calculations. Recently, however, some doubts have arisen: Owocki et al. (1996) suggest a wind-compressed disk may not be formed if the stellar wind is a strong line, radiation-driven wind of the CAK type (Castor et al. 1975). Lamers and Pauldrach (1991) have suggested that the existence of these disks, in general, might be due to the bi-stability mechanism of radiation driven winds. However, they further emphasized that this mechanism is unlikely to be the dominant one for classical Be stars, unless the equatorial mass loss rate is larger than commonly accepted.

An additional simplification, almost always made, has been to bypass the equation for the conservation of energy and instead assume a value, or a simple functional form, for

the kinetic temperature of the circumstellar matter. Klein and Castor (1978) considered the winds of Of stars and showed that, since the radiative terms dominate in the equation for the conservation of energy, the temperature of the circumstellar matter is determined almost completely by the condition of radiative equilibrium. For these spherically symmetric winds, the electron temperature is approximately constant with distance from the star, and slightly smaller than the stellar effective temperature. More recently, Drew (1989) extended the work of Klein and Castor (1978) to include the most abundant heavy elements and found that the electron temperature decreased gradually with increasing radial distance from the star. For disk-like winds, however, the kinetic temperature may vary with position in the disk in a more complex way, because of the two-dimensional character of the density distribution of the circumstellar matter.

In recent years there have been several claims that the energy emitted in lines and continua from the circumstellar envelopes of Be stars is inconsistent with that present in the Lyman and/or Lyman plus Balmer continua of the central star. Ashok et al. (1984) were one of the first to make such a claim. However, van Kerkwijk et al. (1995) noted that this conclusion was incorrect because Ashok et al. had neglected to include the effect of optical depths on line emission. Apparao and Tarafdar (1987) also have asserted that an additional source of high energy photons is needed to account for the observed Balmer line emission, especially for the cooler Be stars. Tarafdar (1994, 1995) has also questioned whether the kinetic temperature assumed for the circumstellar matter in the PM model is too high.

In the remainder of this chapter we first test PM's choice of the kinetic temperature by evaluating the energy gains and losses as a function of position in the circumstellar matter. Then, we determine at each point in the envelope the temperature at which the rates of energy gain and loss are equal.

2.2 The PM Model

One of the ad hoc models for Be stars, the so-called PM model, was introduced by Marlborough (1969) and subsequently modified considerably by Poeckert and Marlborough (1978, hereafter PM). In this model the density of the circumstellar envelope in the equatorial plane at the surface of the star is specified arbitrarily, as is the radial component of velocity in the equatorial plane. The density distribution in the equatorial plane is then determined using the equation of continuity: the density distribution perpendicular to the equatorial plane is assumed to be hydrostatic. Finally the kinetic temperature of the envelope must be chosen: in the PM model the temperature was assumed to be constant, although a simple dependence on distance in the equatorial plane could also have been used.

PM produced a detailed model of this kind for the Be star γ Cas (B0IVe). The stellar mass, radius, effective temperature and log g were chosen to have the values 17 M$_\odot$, 10 R$_\odot$, 25,000 K, and 3.5, respectively. PM assumed a steady state, circumstellar envelope which was symmetric about both the rotation axis and the equatorial plane. The circumstellar matter was assumed to have a kinetic temperature of 20000 K, the latter choice being consistent qualitatively with Klein and Castor (1978).

The ionization-excitation equilibrium was then determined at various locations in a meridional plane by solving the statistical equilibrium equations for the level populations of hydrogen, using both the assumed kinetic temperature of the gas and the local stellar radiation field; the local radiation field is the local value of the photospheric radiation field reduced for both geometrical and physical dilution. We emphasize that no assumption was made in advance concerning the degree of ionization of the circumstellar envelope. Complete details are given by Marlborough (1969), PM and references therein. The shortcomings of the PM model are many; they will not all be enumerated here. Details can be found in Wood et al. (1997), van Kerkwijk et al. (1995), Waters and Marlborough (1994), and references therein.

In the course of our investigations, we discovered and corrected a coding error in one of the subroutines of the original PM code. This error affected the level populations in regions of the envelope where the assumption that the gas is optically thick in all lines was used. Furthermore, PM's choice of 4 grid points perpendicular to the equatorial plane led to inadequate sampling of the exponential density distribution in this direction: we have increased the number of such points to 20. The corrected level populations at each of the grid points tabulated by PM are given in Table 2.1. In Table 2.1, the numbers in brackets refer to the power of 10 by which the entries are to be multiplied. Note that only the populations corresponding to radial distances between 1.50 and 8.00 stellar radii near the equatorial plane have been significantly altered.

Table 2.1: Level Populations for the PM Model. The notation $a(b)$ means $a \cdot 10^b$. Columns (1) and (2) give the radial distance from the central star and the height above the mid-plane, respectively, in stellar radii. Columns (3) to (8) give the densities (in cm^{-3}) of the hydrogen level populations, ground state, 2S, 2P, 3rd, and 4th levels, and the electron density, NE.

r	z	N1	N2S	N2P	N3	N4	NE
1.00	0.00	3.9(09)	1.9(06)	5.7(06)	4.0(06)	4.8(06)	3.3(13)
	0.03	5.8(08)	2.5(05)	7.6(05)	6.0(05)	7.2(05)	1.3(13)
	0.07	2.1(05)	8.4(01)	2.5(02)	2.5(02)	2.5(02)	2.3(11)
	0.10	2.9(02)	7.2(-2)	3.5(-3)	1.3(-2)	2.3(-2)	6.4(09)
1.05	0.00	6.4(10)	6.4(07)	1.9(08)	1.2(08)	1.5(08)	2.5(13)
	0.04	1.5(10)	5.3(05)	1.6(06)	6.3(05)	7.3(05)	7.8(12)
	0.08	2.7(06)	6.6(02)	2.0(03)	1.9(03)	2.1(03)	5.3(11)
	0.12	1.6(03)	2.3(-1)	1.2(-2)	4.3(-2)	7.9(-2)	1.2(10)
1.15	0.00	1.3(13)	5.7(10)	1.7(11)	1.1(11)	1.3(11)	2.6(12)
	0.05	1.5(10)	1.5(06)	4.4(06)	2.0(06)	2.4(06)	7.8(12)
	0.10	7.0(06)	1.3(03)	4.0(03)	3.7(03)	4.1(03)	5.8(11)
	0.15	7.8(03)	6.0(-1)	3.9(-2)	1.3(-1)	2.3(-1)	2.0(10)
1.25	0.00	1.1(13)	6.8(10)	2.0(11)	3.4(10)	3.0(10)	8.3(01)
	0.06	1.2(10)	1.2(06)	3.7(06)	1.7(06)	2.1(06)	5.9(12)
	0.13	1.1(07)	1.6(03)	4.9(03)	4.4(03)	4.9(03)	5.4(11)
	0.19	1.5(04)	8.0(-1)	5.7(-2)	1.8(-1)	3.4(-1)	2.3(10)
1.35	0.00	8.3(12)	3.5(10)	1.1(11)	8.0(10)	1.1(11)	6.8(02)
	0.07	9.1(09)	9.6(05)	2.9(06)	1.3(06)	1.6(06)	4.6(12)
	0.15	1.7(07)	1.7(03)	5.0(03)	4.4(03)	5.0(03)	4.8(11)
	0.22	2.0(04)	8.8(-1)	6.3(-2)	2.0(-1)	3.7(-1)	2.4(10)
1.50	0.00	6.1(12)	5.8(09)	1.8(10)	1.0(10)	1.2(10)	6.5(01)
	0.09	6.6(09)	6.6(05)	2.0(06)	9.1(05)	1.1(06)	3.3(12)
	0.19	3.3(07)	1.6(03)	4.7(03)	4.0(03)	4.5(03)	3.9(11)
	0.28	2.4(04)	8.8(-1)	5.8(-2)	1.8(-1)	3.4(-1)	2.3(10)
1.75	0.00	3.6(12)	1.5(10)	4.4(10)	5.2(10)	5.3(10)	2.4(01)
	0.13	3.4(09)	2.0(05)	6.0(05)	2.4(05)	2.8(05)	1.7(12)
	0.23	7.6(08)	7.1(03)	2.1(04)	7.1(03)	7.8(03)	4.1(11)
	0.36	2.5(04)	7.4(-1)	4.0(-2)	1.2(-1)	2.3(-1)	1.9(10)
2.00	0.00	2.5(12)	2.3(09)	6.8(09)	1.9(10)	3.7(10)	1.6(01)
	0.14	2.9(09)	2.4(05)	7.3(05)	3.2(05)	3.8(05)	1.5(12)
	0.31	3.1(08)	2.1(03)	6.3(03)	2.4(03)	2.6(03)	2.1(11)
	0.45	2.2(04)	6.0(-1)	2.6(-2)	8.1(-2)	1.5(-1)	1.5(10)

Table 2.1: Continued

r	z	N1	N2S	N2P	N3	N4	NE
2.30	0.00	1.5(12)	5.3(08)	1.6(09)	1.3(09)	3.6(10)	1.1(00)
	0.20	1.5(09)	6.4(04)	1.9(05)	7.3(04)	8.4(04)	7.5(11)
	0.38	2.2(08)	1.3(03)	3.8(03)	1.3(03)	1.4(03)	1.3(11)
	0.56	1.4(04)	4.1(-1)	1.2(-2)	3.7(-2)	7.0(-2)	1.0(10)
2.60	0.00	9.8(11)	3.8(09)	1.2(10)	3.9(09)	3.8(09)	2.5(00)
	0.21	1.2(09)	5.9(04)	1.8(05)	6.9(04)	8.0(04)	5.9(11)
	0.45	1.4(08)	7.2(02)	2.2(03)	7.8(02)	8.3(02)	9.1(10)
	0.66	8.7(03)	2.8(-1)	5.9(-3)	1.9(-2)	3.5(-2)	7.3(09)
3.00	0.00	5.9(11)	2.5(09)	7.6(09)	4.8(09)	5.9(09)	6.0(00)
	0.25	7.0(08)	2.8(04)	8.4(04)	3.1(04)	3.6(04)	3.7(11)
	0.51	1.4(08)	8.7(02)	2.6(03)	8.8(02)	9.5(02)	8.1(10)
	0.80	5.1(03)	1.8(-1)	2.6(-3)	8.0(-3)	1.5(-2)	4.8(09)
3.75	0.00	2.7(11)	3.6(08)	1.1(09)	5.8(09)	7.4(09)	4.4(-2)
	0.34	3.3(08)	9.3(03)	2.8(04)	9.9(03)	1.1(04)	1.7(11)
	0.73	4.0(07)	1.9(02)	5.6(02)	1.0(02)	1.9(00)	2.8(10)
	1.06	2.1(03)	9.1(-2)	6.8(-4)	2.1(-3)	4.0(-3)	2.5(09)
4.50	0.00	1.5(11)	6.1(08)	1.8(09)	2.2(09)	4.3(09)	6.2(-2)
	0.42	1.8(08)	3.9(03)	1.2(04)	4.0(03)	4.5(03)	9.7(10)
	0.84	3.4(07)	1.8(02)	5.5(02)	9.8(01)	1.3(00)	2.2(10)
	1.33	1.0(03)	5.1(-2)	2.3(-4)	7.2(-4)	1.4(-3)	1.4(09)
6.00	0.00	6.3(10)	7.8(07)	2.3(08)	1.1(08)	1.6(08)	3.0(-1)
	0.58	7.2(07)	1.1(03)	3.2(03)	1.1(03)	1.2(03)	3.9(10)
	1.27	5.3(06)	2.3(01)	6.9(01)	2.5(00)	5.9(-2)	6.6(09)
	1.85	3.3(02)	2.0(-2)	3.9(-5)	1.3(-4)	2.4(-4)	6.1(08)
8.00	0.00	2.1(10)	1.8(02)	2.7(03)	8.4(02)	1.1(03)	3.(-16)
	0.81	2.3(07)	2.4(02)	7.2(02)	1.6(02)	7.1(-1)	1.3(10)
	1.74	7.5(05)	3.8(00)	1.1(01)	7.7(-2)	5.9(-3)	2.2(09)
	2.55	6.7(01)	6.1(-3)	4.4(-6)	1.5(-5)	2.7(-5)	2.0(08)
12.00	0.00	8.4(06)	4.7(-1)	1.4(00)	7.7(-1)	9.5(-1)	4.9(09)
	1.25	4.9(06)	3.2(01)	9.5(01)	2.6(00)	1.4(-2)	3.0(09)
	2.70	3.7(04)	3.6(-1)	1.1(00)	2.3(-4)	3.1(-4)	5.3(08)
	3.95	8.6(00)	1.2(-3)	2.5(-7)	8.8(-7)	1.7(-6)	5.1(07)

Table 2.1: Continued

r	z	N1	N2S	N2P	N3	N4	NE
16.00	0.00	3.4(06)	4.3(01)	1.3(02)	6.2(00)	7.4(-3)	1.9(09)
	1.69	1.7(06)	7.8(00)	2.4(01)	1.3(-1)	1.7(-3)	1.2(09)
	3.66	1.8(03)	3.5(-2)	8.8(-2)	2.1(-5)	3.3(-5)	2.0(08)
	5.35	2.3(00)	3.9(-4)	3.7(-8)	1.3(-7)	2.5(-7)	2.0(07)
20.00	0.00	1.7(06)	1.7(01)	5.0(01)	9.8(-1)	1.4(-3)	9.9(08)
	2.13	7.9(05)	3.2(00)	9.6(00)	2.1(-2)	4.5(-4)	6.1(08)
	4.62	4.4(02)	9.6(-3)	1.8(-2)	4.8(-6)	8.2(-6)	1.1(08)
	6.75	9.7(-1)	1.8(-4)	1.0(-8)	3.7(-8)	7.0(-8)	1.0(07)
28.00	0.00	5.5(05)	4.7(00)	1.4(01)	1.0(-1)	2.2(-4)	4.1(08)
	3.02	3.0(05)	1.0(00)	3.1(00)	2.2(-3)	7.8(-5)	2.5(08)
	6.53	1.0(02)	2.5(-3)	2.7(-3)	7.6(-7)	1.4(-6)	4.5(07)
	9.55	3.4(-1)	6.3(-5)	1.8(-9)	6.6(-9)	1.2(-8)	4.4(06)
36.00	0.00	2.4(05)	1.6(00)	4.9(00)	1.5(-2)	5.5(-5)	2.1(08)
	3.90	1.4(05)	4.3(-1)	1.3(00)	1.6(-5)	2.1(-5)	1.3(08)
	8.45	3.9(01)	1.0(-3)	6.0(-4)	1.9(-7)	3.6(-7)	2.3(07)
	12.35	1.5(-1)	2.9(-5)	5.(-10)	1.8(-9)	3.3(-9)	2.3(06)
50.00	0.00	1.0(05)	6.0(-1)	1.8(00)	2.4(-3)	1.3(-5)	1.0(08)
	5.45	7.1(04)	1.7(-1)	5.1(-1)	3.5(-6)	4.6(-6)	6.2(07)
	11.80	1.6(01)	4.3(-4)	1.4(-4)	4.4(-8)	8.2(-8)	1.1(07)
	17.25	6.5(-2)	1.2(-5)	1.(-10)	4.(-10)	8.(-10)	1.1(06)
75.00	0.00	4.5(04)	2.2(-1)	6.6(-1)	4.1(-4)	2.5(-6)	4.5(07)
	8.21	3.5(04)	5.6(-2)	1.7(-1)	6.1(-7)	8.3(-7)	2.8(07)
	17.79	5.8(00)	1.8(-4)	3.2(-5)	8.5(-9)	1.6(-8)	4.9(06)
	26.00	2.9(-2)	5.3(-6)	2.(-11)	8.(-11)	2.(-10)	4.8(05)

2.3 Energy Gains and Losses of the PM Model

We assume that the gas dynamical terms in the equation for the conservation of energy are sufficiently small that the gas in the circumstellar envelope can be assumed to be in radiative equilibrium, so that at each point in the envelope the radiative heating and cooling rates balance. Klein and Castor (1978) demonstrated that this assumption was a good one for the rapidly expanding, Of star winds they investigated. In the PM model the radial component of velocity of the circumstellar matter is considerably smaller and the particle density generally larger than the same quantities in the Of star winds, so our assumption is expected to be valid at least for the equatorial regions of the circumstellar envelopes of Be stars. It may also be a reasonable assumption for the bulk of the circumstellar envelope.

At any point in the circumstellar envelope, a variety of processes at the microscopic level convert energy in the form of radiation into internal and/or thermal energy of the gas and vice-versa. Free electrons in a unit volume of gas gain energy from photoionization, collisional deexcitation of bound levels and free-free absorption; electrons lose energy by recombination, collisional excitation and free-free emission. The PM model requires that a gas temperature be specified initially. We can evaluate the rates of energy conversion, determine their ratio at each grid location and compare this ratio to unity. If, by chance, the correct temperature were assumed, this ratio would be unity at each location. If the ratio is not unity at a specific grid point, the choice of temperature at that grid point was not correct. An average of this ratio for all grid points permits us to assess the validity of the isothermal envelope temperature of 20,000 K assumed by PM. Also, by determining this ratio at each grid point considered in the envelope, the temperature there at which the rates balance can be determined iteratively. In the following subsection we describe the procedures by which each of these rates of energy conversion was evaluated.

2.3.1 Energy Rate Calculations The energy gain per electron from photoionization, $E_{n,\kappa}$, was determined by multiplying the integrand of the standard integral used to

determine the number of photoionizations from level n per unit volume per unit time per particle by $h(\nu - \nu_n)$.

$$E_{n,\nu} = \int_{\nu_n}^{\infty} \frac{c}{h\nu} h(\nu - \nu_n)\, a_n(\nu)\, u_\nu d\nu, \tag{2.1}$$

where ν_n is the series limiting frequency for photoionization from level n, c is the speed of light, $a_n(\nu)$ is the cross-section for photoionization at frequency ν, u_ν is the energy density of radiation at frequency ν and h is Planck's constant. The same numerical scheme employed in the PM model to evaluate the photoionization rate was used to evaluate this integral.

The energy emitted due to capture of electrons to level n per unit volume per unit time is given by,

$$R_{\nu,n} = \frac{4\pi}{c^2} N_e N_+ \left(\frac{g_+}{g_n} \frac{(2\pi m_e kT)^{\frac{3}{2}}}{h^3} \right)^{-1} \exp\left(\frac{I_n}{kT}\right) \times \int_{\nu_n}^{\infty} \nu^2 h(\nu - \nu_n)\, a_n(\nu) \exp(-\frac{h\nu}{kT}) d\nu, \tag{2.2}$$

where c is the speed of light, m_e is the mass of the electron, k is the Boltzmann constant, N_e is the number density of free electrons, N_+ is the number density of ions, I_n is the minimum ionization energy from level n, and $a_n(\nu)$ is the cross-section for photoionization at frequency ν from level n. A 7 point, Gauss-Laguerre integration scheme was used to evaluate this integral.

A radiative excitation of a bound electron followed by a collisional de-excitation represents a net energy gain by the electron gas. Conversely, a collisional excitation followed by a radiative de-excitation will result in an energy loss. Therefore, if one knows the population of a particular level, the number density of free electrons, the collisional transitional rates, and the difference in energy of the two levels involved in the transition, then the losses and gains of energy of the electron gas due to transitions between bound levels can easily be

calculated. Note that in the PM model only collisional transitions which involved a change in the principle quantum number of ± 1 were considered. We will consider only these same transitions in this thesis.

The energy loss by free-free emission or bremsstrahlung can easily be calculated using the standard expression. (Osterbrock 1974). Alternatively, a free electron may absorb a photon and make a transition to a higher state which increases the energy of the gas, that is free-free absorption or inverse bremsstrahlung (Tucker 1975). These free-free terms are not expected to be dominant contributors to the energy gains and losses but have been included for completeness.

2.4 Results The equations used to determine the energy losses and gains depend explicitly in a non-linear way on temperature and also have an additional complex, implicit dependence on temperature through the level populations. If the assumed temperature of the envelope at a given grid point were exactly correct, the rate of energy gain per unit volume divided by the rate of energy loss at that location would be exactly 1. In considering the original isothermal case, we have used the ab initio assumption for the temperature of 20,000 K made by PM. A simple global average of the ratio of energy gain to loss for this 20,000 K, isothermal model is 0.6 ± 0.3 (1σ); a density weighted average of the same ratio is 0.76 ± 0.02 (1σ). The density weighted average is dominated by regions of the envelope near both the star and the equatorial plane where densities are high. We conclude that the temperature assumed by PM was a reasonable first order approximation.

In order to determine the temperature corresponding to equal rates of energy gain and loss, the PM code was modified to permit the electron temperature to be a function of position. An initial guess for the temperature grid was determined in the following manner. The ratio of the rate of energy gain to loss was computed at each grid point for isothermal model envelopes characterized by a specific choice for the kinetic temperature of the gas. This process was then repeated for a range of kinetic temperatures. Therefore, at each grid

point a series of such ratios was obtained: each ratio corresponds to a particular constant temperature envelope. At each grid point, interpolation among the set of energy ratios yielded the temperature required for equal rates of energy gain and loss. Subsequently, this temperature grid was used as an initial guess for the temperature. Then the ionization-excitation program was run, level populations recalculated, and a new energy ratio was determined at each grid position. The temperature was re-adjusted at individual grid points and ionization-excitation program was rerun until the ratio of energy gain to loss at each grid point differed from unity by less than some prescribed amount. Varying the temperature at a grid point changed the ratio of gain to loss by an amount that depended on the processes that were dominant at that particular position. Experience allowed one to determine whether to increase or decrease the temperature at a particular grid point, depending on the value of the ratio there. Temperature adjustments were made in steps of at least 500 K. This iterative process was repeated until the standard deviation of the energy ratios in the final solution was ≤ 0.01 for consistency. However, individual temperatures are certainly not this accurate. The error of the level populations is at least 5% due to the manner in which they are determined. We have not attempted to assign absolute errors to the predicted temperatures due to the uncertainties in many of the parameters used. Nevertheless, the resulting temperature grid does represent a consistent solution for which the equation of energy conservation is satisfied.

The number of grid points in the z direction, each of which is referred to by its J value with J = 1 in the equatorial plane, was increased from 4 equally spaced points in the original PM model to 20 grid points, spaced unequally in order to sample better the exponential density decrease in the PM model perpendicular to the equatorial plane. Thus there are 480 grid points, 20 J values for each of the 24 ϖ values. At positions in the envelope corresponding to J = 20 (J = 4 in the PM model), it was assumed that there was no material above these locations. This assumption is unphysical since there will certainly be some material beyond these positions. Therefore, the grid points corresponding to J = 20 were excluded from the final analysis.

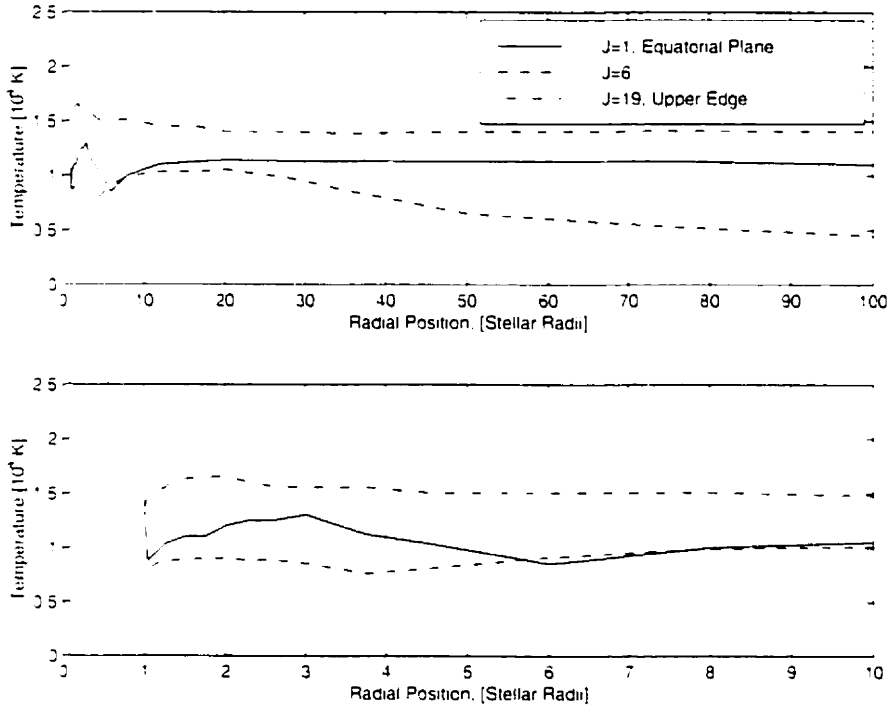

Figure 2.1: The temperature for which the energy gain balances the energy loss as a function of distance from the rotation axis for three locations in the circumstellar envelope: the equatorial plane (J=1), an intermediate location (J=6), and the upper edge (J = 19).

A simple global average of the energy ratios corresponding to the set of final temperatures is 1.00 ± 0.01 (1σ). This demonstrates that the rates of energy gain and energy loss are balanced throughout the envelope. A density weighted average of the energy ratios corresponding to the set of final temperatures is 1.01 ± 0.01 (1σ). This result is dominated by the energy ratios in the equatorial plane where densities are high. See Figure 2.1 for a graph of temperature versus radial position in the equatorial plane, at the upper edge, and at an intermediate position. The portion of the envelope nearest the star has been expanded in the lower part of the figure to resolve temperature variations more easily. The J = 19 position varies from a height of 0.10 stellar radii above the equatorial plane at the surface of the star to a height of 34.40 stellar radii at a radial distance of 100 stellar radii. The J = 6 position, referred to in Figure 2.1, corresponds to a height of 0.03 stellar radii at the stellar surface, a height of 1.19 stellar radii at a radial distance 12 stellar radii, and increases to a height of 10.4 stellar radii at a radial distance of 100 stellar radii; these positions correspond to scale heights of 0.9, 0.4, and 0.4, respectively. The temperature curves are relatively flat except for distances within 6 stellar radii of the star's surface. It is apparent that temperatures within the envelope are strongly dependent on the height above the equatorial plane.

It should be emphasized that there is not a monotonic increase in temperature between the equatorial plane and the upper edge of the envelope. In the upper portions of the envelope, energy gains and losses are dominated by radiative processes, in particular, photoionization and radiative recombination. Along the equatorial plane, collisional processes dominate the energy terms out to a distance of approximately 4.5 stellar radii. In fact, the most conspicuous feature in Figure 2.1 is a temperature increase and subsequent decrease of approximately 5,000 K in the equatorial plane between 1 and 5 stellar radii where collisional processes dominate. Between 4.5 and 8 stellar radii, collisional energy terms are the same order of magnitude as the radiative terms. At increasing heights above the equatorial plane, the temperature structure is quite complicated because collisional terms gradually decrease in importance as the particle number density decreases. Generally, the tempera-

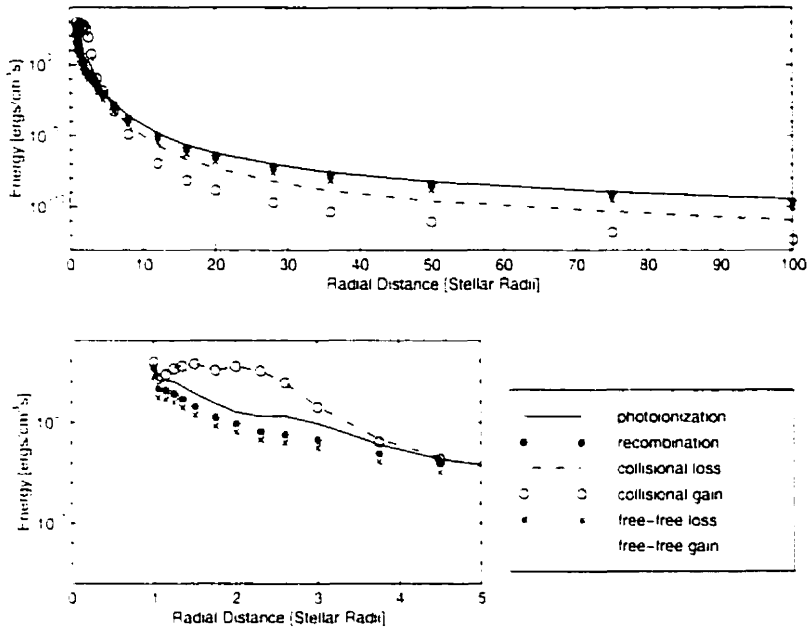

Figure 2.2: The sources of energy gain and loss along the equatorial plane (J=1).

ture decreases with increasing height above the equatorial plane because the energy density of radiation remains low and collisions become less important as number densities decrease exponentially. See Figure 2.1, J = 6. Further from the equatorial plane the temperature begins to increase as energy densities increase since the envelope gradually becomes optically thin in the continuum.

The envelope is almost completely ionized everywhere. However, over a small region in the equatorial plane near the star the degree of ionization is reduced. At a radial distance of 1.05 stellar radii up to a height above the plane of 0.05 stellar radii and out to 2.6 stellar radii up to a height of 0.03 stellar radii, the degree of ionization varies between 45 and 75 percent. In this region the temperature is approximately 15,000 K: see Figure 2.1. The original PM model assumed a constant temperature of 20,000 K and the gas was largely ionized. In the corrected PM model, between radial distances of 1.15 and 8.0 stellar radii up to a maximum height of 0.14 stellar radii from the equatorial plane, the envelope is largely neutral: see Table 2.1. The cause of the lower degree of ionization, in a larger region, at a higher temperature in the corrected PM model compared with the variable temperature

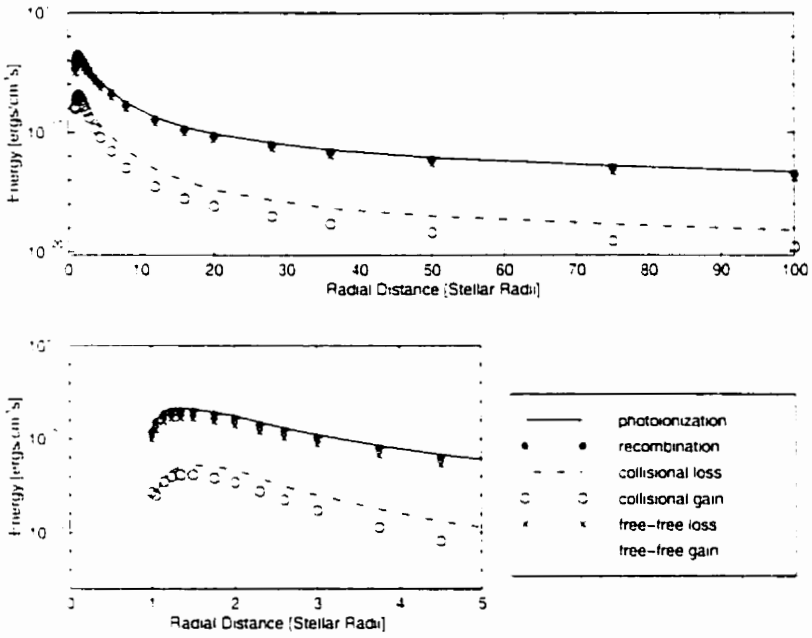

Figure 2.3: The same as Fig. 2.2 for the upper envelope (J=19).

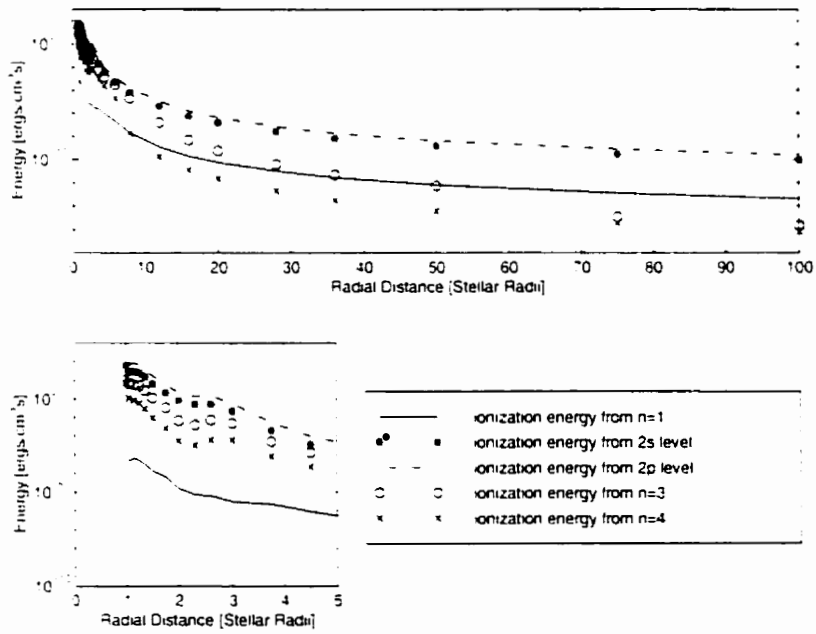

Figure 2.4: The contribution of ionization energy from levels n = 1, 2s, 2p, 3, and 4 for the equatorial plane (J=1).

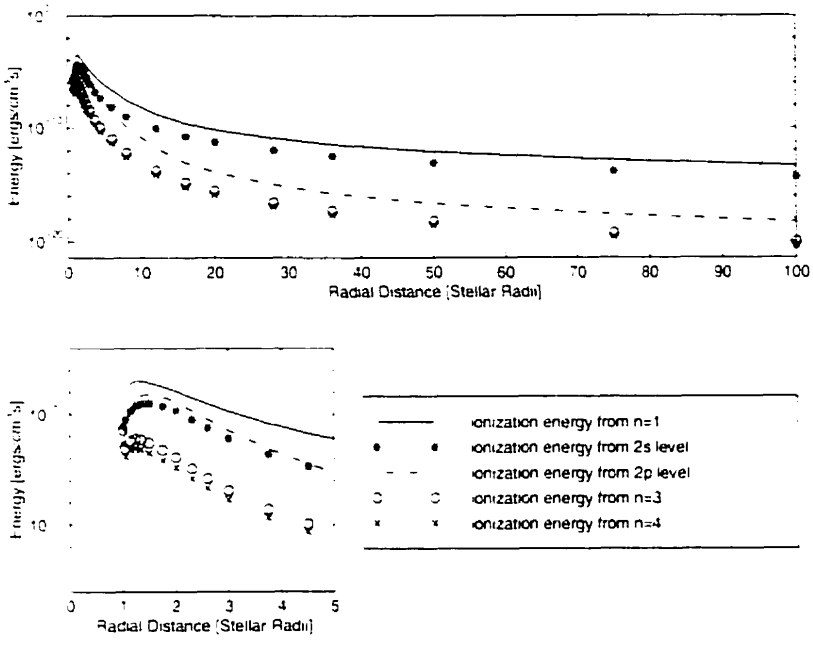

Figure 2.5: The same as Fig. 2.4 for the upper envelope (J=19).

model is straight forward. Here the envelope is optically thick in all line radiation in both models. In addition, the collisional transition probabilities between bound levels are strongly sensitive on temperature. At higher temperatures, collisions populate the upper levels more effectively. This results in larger column densities at frequencies corresponding to photoionization from these upper levels and these large column densities decrease the energy density of stellar radiation reaching these locations. Consequently, the probability of photoionization per particle is reduced; hence the envelope becomes neutral. The variation in the degree of ionization between these models, which have a difference of only 5,000 K in temperature in this particular region of the envelope, further illustrates the need to have a self consistent solution for which the equation of energy conservation is satisfied.

In the equatorial plane, at distances greater than 5 stellar radii, photoionization and radiative recombination are the dominant energy terms. At distances within 5 stellar radii collisional processes dominate the energy terms. Collisions dominate where number densities are large. In the equatorial plane near the star number densities are of the order $10^{13}\,\mathrm{cm}^{-3}$.

Figure 2.2 shows the relative importance of the energy terms in the equatorial plane. Beyond a distance of 4.5 stellar radii, the collisional terms cease to be the dominant energy terms. In fact, even within 8 stellar radii, at heights greater than approximately 0.6 stellar radii above the equatorial plane, radiative terms dominate. Figure 2.3 shows the relative importance of the energy terms along the upper edge of the envelope. As expected, radiative terms dominate at all radial distances.

Figures 2.4 and 2.5 show the relative importance of photoionization from levels, n = 1, 2s, 2p, 3, and 4 along the equatorial plane and along the upper edge of the envelope. In the equatorial plane near the star, the densities are high and the envelope is optically thick in line radiation. Collisional processes and scattered line radiation result in increased populations above the ground state and radiation is available in the Balmer and longer wavelength continua to ionize the atoms. Consequently, photoionization from the 2p and n = 3 levels contributes the most energy input to the envelope in the equatorial plane. Photoionization from n = 1 is substantially reduced between radial distances of 1.05 and 8.0 stellar radii where the envelope is not completely ionized. Further from the equatorial plane, the envelope more closely resembles a nebula, with most of the ionization coming from the ground state.

2.5 Discussion

It is evident from a consideration of either the simple global average or the density weighted average of the ratio of energy gain to loss that PM's choice of a constant kinetic temperature of 20,000 K was a reasonable, first order approximation for the temperature of the circumstellar envelope of γ Cas. Nevertheless, as shown in Figure 2.1, the kinetic temperature does have a moderately strong positional dependence so that the assumption of a constant kinetic temperature is at best a first order approximation. More realistic models for the circumstellar matter around Be stars and similar objects will by necessity have to include the dependence of kinetic temperature on position in the envelope.

The modified PM model described in this thesis represents the first such approach of which we are aware.

Several assumptions were used in evaluating the ionization-excitation equilibrium in the PM model. We review these here in order that the reader can judge the appropriateness or otherwise of the approximations used and therefore the accuracy of the temperature structure of the envelope we have obtained. The procedure to obtain the ionization-excitation conditions was described by Marlborough (1969) and PM. Several simplifying assumptions were made, which affect the determination of the kinetic temperature. First, the contribution of the diffuse radiation field to the local continuum background was neglected in evaluating the photoionization rates from each bound level. By neglecting the diffuse radiation field we have underestimated both the degree of ionization and the local electron temperature, because the capture of a free electron to the ground state, for example, yields a Lyman continuum photon which can subsequently photoionize a hydrogen atom and, more importantly, heat the gas. Inclusion of the diffuse field will have a more significant effect where the gas is cooler and has a lower degree of ionization, specifically those parts of the envelope near the equatorial plane and between 1 and 3 stellar radii from the surface of the star. One expects both the degree of ionization and the temperature of the gas in this region of the envelope to be somewhat higher than our predictions when the diffuse radiation field is included.

Second, only collisional transitions between levels n and n±1 were included in the statistical equilibrium equations. This simplification is satisfactory for collisional excitations because the increasing energy threshold reduces the importance of transitions from n to n−2, n−3, etc, compared to the transition n to n−1. A similar simplification is appropriate for collisional de-excitation because the transition n to n-1 has a higher rate coefficient than n to n-2, etc.

Third, a simple approximation was used to evaluate the local energy density of line radiation; it is described in detail by Marlborough (1969). Essentially this procedure as-

sumes that the energy density of radiation in each line, or equivalently the level populations including the effects of the local radiation field in the lines, can be obtained using the local ionization-excitation equilibrium assuming a particular series of lines is either optically thick or thin, together with the optical depth in line radiation along a path, parallel to the rotation axis, from the grid point at which the ionization-excitation conditions are being determined to the upper boundary of the envelope. This approach avoids the necessity of determining the constant velocity surfaces in the rotating, expanding wind, which are needed to use the Sobolev approximation. The justification for this approximation is the degree to which the PM model reproduced satisfactorily the observational data for γ Cas.

Our investigation has shown that it is possible, given a background density and velocity distribution for the circumstellar envelope, to determine self-consistently both the ionization-excitation equilibrium and the electron temperature distribution as a function of position in the circumstellar envelope. Therefore we have eliminated the necessity to assume arbitrarily the kinetic temperature of the gas in the circumstellar envelope.

The variation of the kinetic temperature with position may produce ionization gradients within the circumstellar envelope. In the case of an early B star, for example, for which the PM model may be a reasonable approximation for the structure of the circumstellar envelope, Fe II might be the dominant stage of ionization of iron in the cooler parts and Fe III dominant in the hotter regions. If this possibility is confirmed, metal lines from different stages of ionization may prove to be valuable probes of the physical conditions in the circumstellar regions of the hotter Be stars. This might also help to resolve the controversy concerning the location of the region where shell lines form and the electron number density there (Hubert 1994).

We are considering extending this analysis to the disk model (Waters 1986, Waters et al. 1987) in a subsequent chapter. The results of these analyses will be used to construct an improved model. These improvements will include changes to the density distribution above the equatorial plane and flexibility to allow the upper edge of the envelope to vary in shape.

Bibliography

Apparao, K. M. V. & Tarafdar, S. P., 1987. *ApJ* **322**, 976.

Ashok, N. M., Bhatt, H. C., Kulkarni, P. V., & Joshi, S. C., 1984. *MNRAS* **211**, 471.

Balona, L. A., Henrichs, H. F., & Contel, J. M. L. (Eds.), 1994. *IAU Symp. 162, Pulsation, Rotation and Mass Loss in Early-Type Stars*. Dordrecht: Reidel.

Bjorkman, J. E. & Cassinelli, J. P., 1993. *ApJ* **409**, 429.

Castor, J. I., Abbott, D. C., & Klein, R. I., 1975. *ApJ* **195**, 157.

Coyne, G. V. & McLean, I. S., 1982. In M. Jaschek and H. G. Groth (Eds.), *IAU Symp. 98, Be Stars*. Reidel, Dordrecht.

Dougherty, S. M. & Taylor, A. R., 1992. *Nature* **359**, 808.

Drew, J. E., 1989. *ApJS* **71**, 267.

Hubert, A. M., 1994. In L. A. Balona, H. F. Henrichs, and J. M. L. Contel (Eds.), *IAU Symp. 162, Pulsation, Rotation and Mass Loss in Early Type Stars*. Reidel, Dordrecht.

Klein, R. I. & Castor, J. I., 1978. *ApJ* **220**, 902.

Lamers, H. J. G. L. M. & Pauldrach, A. W. A., 1991. *A&A* **244**, L5.

Marlborough, J. M., 1969. *ApJ* **156**, 135.

Marlborough, J. M., 1976. In A. Slettebak (Ed.), *IAU Symp. 70, Be and Shell Stars*. Reidel, Dordrecht.

Marlborough, J. M., 1987. In A. Slettebak and T. P. Snow (Eds.), *IAU Symp. 92, Physics of Be Stars*. Cambridge, Cambridge University Press.

Osterbrock, D. E., 1974. *Astrophysics of Gaseous Nebulae*. U.S.A.: W.H. Freeman and Company.

Owocki, S., Cranmer, S. R., & Gayley, K. G., 1996. *ApJ* **472**, L115.

Owocki, S., Cranmer, S. R., & M.Blondin, J., 1994. *ApJ* **424**, 887.

Poeckert, R. & Marlborough, J. M., 1978. *ApJ* **220**, 940. (PM).

Quirrenbach, A., Bjorkman, K. S., Bjorkman, J. E., Hummel, C. A., Buscher, D. F., Armstrong, J. T., Mozurkewich, D., H. N. M. E., & Babler, B. L., 1997. *ApJ* **479**, 477.

Quirrenbach, A., Hummel, C. A., Buscher, D. F., Armstrong, J. T., Mozurkewich, D., & H. N. M. E., 1993. *ApJ* **416**, L25.

Slettebak, A. & Snow, T. P. (Eds.), 1987. *IAU Symp. 92, Physics of Be Stars*. Cambridge: Cambridge University Press.

Stee, P., de Araújo, F. X., Vakili, F., Mourard, D., Arnold, L., Bonneau, D., Morand, F., & Tallon-Bosc, I., 1995. *A&A* **300**, 219.

Tarafdar, S. P., 1994. *private communication*.

Tarafdar, S. P., 1995. *private communication*.

Tucker, W. H., 1975. *Radiation Processes in Astrophysics*. Cambridge: M.I.T. Press.

Underhill, A. B. & Doazan, V., 1982. *B Stars With and Without Emission Lines*. U.S.A.: NASA SP-465.

van Kerkwijk, M. H., Waters, L. B. F. M., & Marlborough, J. M., 1995. *A&A* **300**, 259.

Waters, L. B. F. M., 1986. *A&A* **162**, 121.

Waters, L. B. F. M., Coté, J., & Lamers, H. J. G. L. M., 1987. *A&A* **185**, 206.

Waters, L. B. F. M. & Marlborough, J. M., 1994. In L. A. Balona, H. F. Henrichs, and J. M. L. Contel (Eds.), *IAU Symp. 162, Pulsation, Rotation and Mass Loss in Early-Type Stars*. Reidel, Dordrecht.

Wood, K., Bjorkman, K. S., & Bjorkman, J. E., 1997. *ApJ* **477**, 926.

Chapter 3

1 Delphini[2]

3.1 Introduction We have investigated the rates of energy gain and loss in the circumstellar envelope of the cool B8-9e star, 1 Del, using the PM model. We determined iteratively the kinetic temperature of the gas as a function of position in the circumstellar envelope by adjusting the temperature at each grid point until the rates of energy gain and loss there were equal. The gas was assumed to gain energy from photoionization, collisional de-excitation of bound levels and free-free absorption, and to lose energy by recombination, collisional excitation and free-free emission. The resultant temperatures are a self-consistent solution of the equation of energy conservation. We were also able to reproduce the gross features of the Hα line with this model and the corresponding temperature grid. Our investigation demonstrates that there is sufficient continuum radiation present to ionize the circumstellar envelope and produce the relative line strength without any additional source of heating in the envelopes of cool Be stars.

Be stars are observed to exhibit emission in one or more Balmer lines, typically Hα, at some time. Generally, the strength of the Balmer emission decreases for later spectral types. Emission may also be present in lines of He I and also in lines of singly ionized metals, for example, Fe II. These stars also are observed to have excess continuum radiation both in the infrared and at longer wavelengths. The Be stars which have sharp deep absorption

[2]A version of this chapter has been published: Millar C. E., Marlborough J. M., (1999) Rates of energy gain and loss in the circumstellar envelopes of Be stars: 1 Delphini, ApJ, 516, 280.

cores in the spectral lines of hydrogen and singly ionized metals, are commonly called shell stars.

The gas in which the emission lines and excess continuum radiation arise is generally considered to be the denser parts of a disk-like stellar wind, which is concentrated both toward the star and toward the equatorial plane. Spectroscopic data indicate that there is a two component nature to this wind: analysis of UV spectra suggests a low density polar wind with outflow velocities of several hundreds km/s, while from optical spectra a high density equatorial wind with very low outflow velocities is inferred. Be stars also have a high intrinsic linear polarization which further implies a non-spherical distribution of gas. See review articles in Slettebak and Snow (1987), Balona et al. (1994), and references therein. Recently, support for a flattened equatorial distribution of gas has come from direct imaging, Dougherty and Taylor (1992), Quirrenbach et al. (1993), and Stee et al. (1995).

It has been suggested that the continuum and line radiation from the central star is not sufficient to ionize the circumstellar envelope and produce the energy emitted in lines and continua in the envelope of all Be stars, but especially for the later types (Ashok et al. 1984, Apparao and Tarafdar 1987, 1997a, 1997b). In an earlier chapter, (Millar and Marlborough 1998, hereafter MM), we determined in a self consistent manner the kinetic temperature of the gas in the circumstellar envelope for the early Be star, γ Cas, using the model of Poeckert and Marlborough (1978), hereafter PM. The kinetic temperature was determined from the requirement that the rates of energy gain and loss at each point in the circumstellar envelope be equal. Photoionization, collisional de-excitation of bound levels and free-free absorption were assumed to contribute to the rate of energy gain: radiative recombination, collisional excitation of bound levels and free-free absorption contribute to the rate of energy loss. For additional details see MM.

In this chapter we extend our analysis of the PM model to include a cool Be star in order to investigate further the claim of Apparao and Tarafdar (1987, 1997a, 1997b). The energy rate calculations and corresponding temperatures within the circumstellar envelope

are given here for the star 1 Del. This star has a spectral type in the range B8-9 e-shell (Slettebak and Carpenter 1983): it was previously modeled by Marlborough and Cowley (1974), hereafter MC.

3.2 The Model

There are some substantial differences between the models used by MC, PM, and the model of MM used here. The model used by MC was based on the work of Marlborough (1969): the model used here, although based on the same work, was substantially modified by PM. An error in both the model used by MC and the model used by PM was corrected by MM: see MM for details.

The envelope is assumed to be symmetric about both the rotation axis of the star and the equatorial plane. The central star is assumed to be spherically symmetric and rotating at the Keplerian speed. The maximum height of the envelope above the equatorial plane varies from 0.1 stellar radii at the stellar surface to a height of 34.75 stellar radii at a radial distance of 100 stellar radii. Beyond this maximum height of the envelope, the envelope density was assumed to be zero. The specific choice of this maximum height of the envelope does not influence our results in any significant way because of the exponential decrease of density with increasing distance perpendicular to the equatorial plane.

The stellar mass, radius, effective temperature and log g were assumed to have the values 4 $M_\odot$, 3.3 $R_\odot$, 12,600 K, and 4, respectively, identical to those used by MC. The number density at a position in the equatorial plane and the velocity distribution in the radial direction are assumed; then the equation of continuity is solved for the density distribution in the equatorial plane. The assumed outflow velocities at radial distances of 1, 5, 15, 20, and 400 stellar radii were 1, 5, 7, 15, and 60 km s^{-1}, respectively; this is also identical to that adopted by MC. We used an assumed number density of 4.19×10^{13} cm^{-3} at a radial distance of 4 stellar radii; MC used a value of 2.35×10^{12} cm^{-3} at this position. The value of the number density was chosen in order to reproduce the gross features of the Hα line. It is not surprising that the density used here is quite different from MC. The model used by

MC is substantially different from the current model. In particular, the model used by MC had a coding error in one of the subroutines. This error affected the level populations in regions of the envelope where the gas was assumed to be optically thick: this is discussed in MM. In addition, many improvements and additions have been made to this code by PM since it was used by MC.

At a specified location in the equatorial plane, ω', the density distribution perpendicular to the equatorial plane is assumed to be hydrostatic: this sets the position and shape of the projection of the density streamlines in a meridional plane. As the value of this parameter increases, the emitting volume of the envelope also increases. We have used the value of $\omega' = 4$, the same as that used by MC. The particular combination of the assumed parameters allowed us to reproduce satisfactorily the gross features of the H_α line: see Figure 3.1. The predicted line has roughly the correct amount of emission and the widths of the observed and predicted lines are quite similar. However, there are some differences in detail, especially in the shape of the line wings. Nevertheless, since the main objective of this exercise was to check to validity of the temperature previously assumed for the envelope by MC and further to determine a self-consistent temperature profile, we were satisfied to reproduce only the gross features of the Hα line. It should also be noted that the observed line in Figure 3.1 is an average of a series of observations recorded on photographic plates: see Fig. 1 of MC. Uncertainties arising from the conversion of photographic density to relative line strength, together with the fact that Be star spectra are variable, suggests that trying to match observation and model exactly may be futile.

3.3 Results

The kinetic temperature derived from the criterion of equal rates of energy gain and loss is shown in Figure 3.2 as a function of radial distance in the equatorial plane, at a position half way between the equatorial plane and upper edge, and at the upper edge of the envelope. Since there is an exponential decrease in the density distribution perpendicular to the equatorial plane, most of the material in a particular column lies

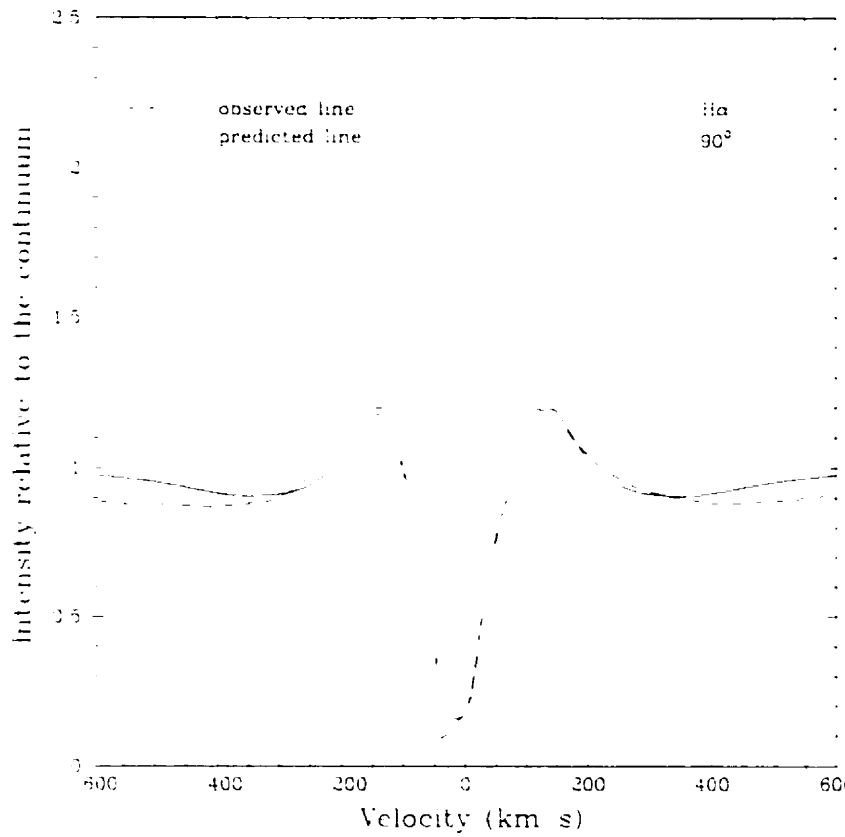

Figure 3.1: Predicted H α line derived from the model calculations compared to the observed line. The model assumes the disk is viewed edge on, that is, at an inclination angle of 90°.

below a position half way between the equatorial plane and the upper edge. For example, at a radial distance of 1 stellar radii at J = 10, 0.0474 stellar radii above the equatorial plane, with the point corresponding to J = 1 being in the equatorial plane, 99.8% of the material in a column which extends to the upper edge lies below this position. Similarly, at a radial distance of 34.75 stellar radii at J = 10, 16.46 stellar radii above the equatorial plane, 99.6% of the material in a column which extends to the upper edge lies beneath this position. The global average kinetic temperature for this model is 5800±1000 K (1σ); the density weighted average is 5900±40 K (1σ). The difference of these two average temperatures reflects the fact that the kinetic temperature is higher in the equatorial plane where the density is higher. The kinetic temperature remains fairly constant with increasing radial distance from the star, and is essentially isothermal. The temperature of the upper edge of the envelope, however, is approximately 1000 K cooler than the mid-section of the disk. Near the equatorial plane, as the density increases collisional processes become increasingly important and tend to populate upper levels. Consequently, even though the envelope is optically thick to Lyman continuum photons, photoionization from upper levels is able to heat the gas.

The radial dependence of processes which contribute to energy gains and losses is shown in Figure 3.3 and Figure 3.4 as a function of distance from the star for the equatorial plane and upper edge, respectively. The dominant source of energy gain and loss at almost all locations in the envelope is photoionization and radiative recombination, respectively. Collisional processes dominate in a very small region in the equatorial plane between the stellar surface and a radial distance of 1.05 stellar radii. Collisional processes are only important where both the density and temperature are large. At radial distances greater than 1.05 stellar radii, energy gain from photoionization has the largest absolute value of all the heating and cooling terms. From the radial distance of 1.05 to 1.80 stellar radii in the equatorial plane, the rate of energy loss due to collisions is larger than the recombination energy rate. However, at all other locations the photionization and radiative recombination terms are the largest. See Figure 3.3.

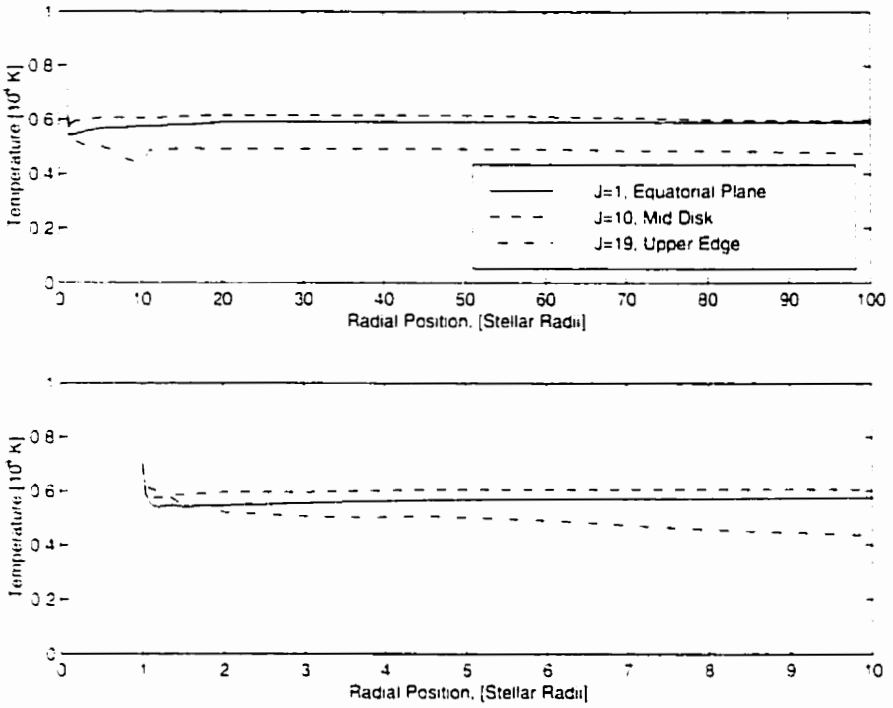

Figure 3.2: The temperature for which the energy gain balances the energy loss as a function of distance from the rotation axis for three locations in the circumstellar envelope: the equatorial plane (J=1), an intermediate location (J=10), and the upper edge (J = 19).

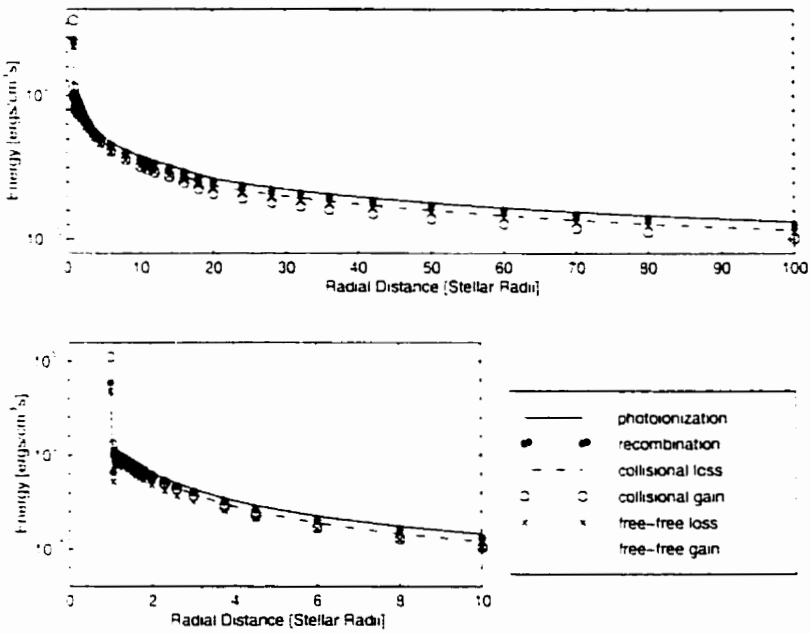

Figure 3.3: The sources of energy gain and loss along the equatorial plane (J=1).

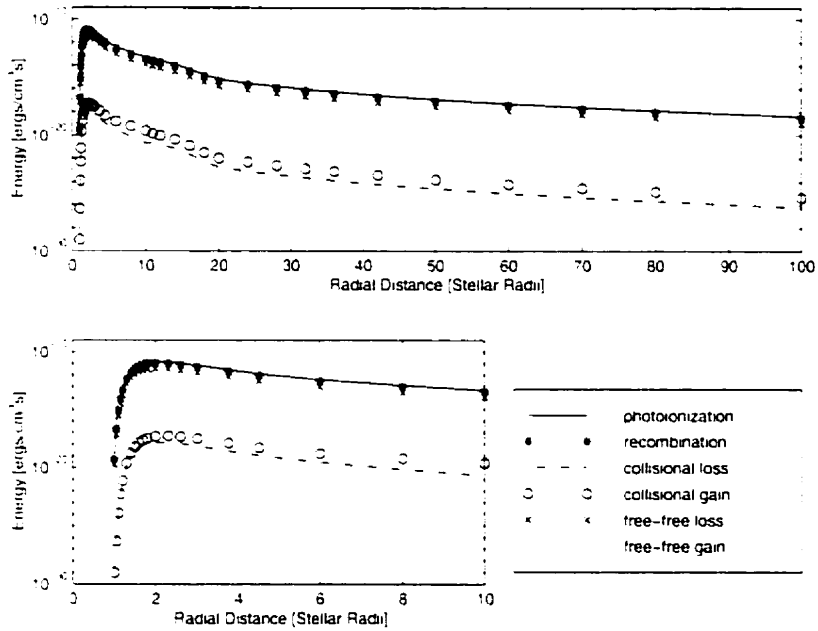

Figure 3.4: The same as Figure 3.3 for the upper envelope (J=19).

Nevertheless, near the star and in the equatorial plane where densities are the greatest, collisions are important in increasing the populations above the ground level from which atoms may then be photoionized. Along the upper edge where densities are low, collisional energy terms are orders of magnitude smaller than photoionization and recombination energy terms; see Figure 3.4.

Energy transfer to the gas in the equatorial plane is dominated by photoionization from levels 2p and 2s. In the equatorial plane the gas is optically thick in Lyman continuum radiation; consequently photoionization from level 1 by stellar radiation is not important. In contrast, the upper edge of the envelope is dominated by photoionization from levels 1 and 2s. The heating due to photoionization from level 2s is important here due to the relative increase in the population of this meta-stable level. The number density is low along the upper edge and collisions are not important; consequently the population in level 2s becomes substantially greater than the population in 2p. When collisions are dominant the population in level 2p is expected to be approximately 3 times the population in level 2s.

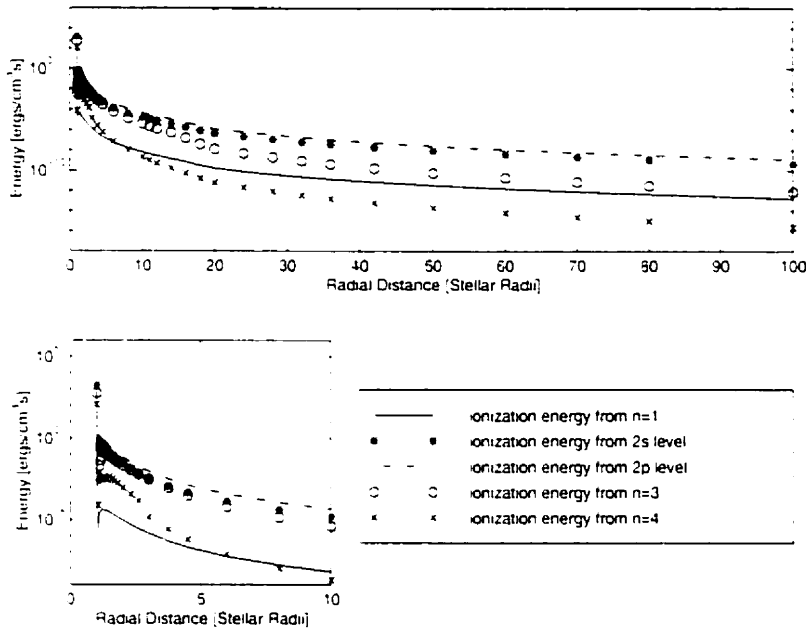

Figure 3.5: The contribution of ionization energy from levels n = 1, 2s, 2p, 3, and 4 for the equatorial plane (J=1).

See Figure 3.5 and Figure 3.6 for graphs of the source of photoionization energy as a function of radial distance from the star for the equatorial plane and upper edge, respectively.

The portion of the envelope nearest the equatorial plane is neutral. The greatest degree of ionization in the equatorial plane is 1.3% near the star, at all other radial distances in the equatorial plane, the degree of ionization is less than this value. There is simply not enough ionizing radiation from the star able to reach the dense areas to keep the gas ionized. With increasing height above the equatorial plane, the ionization fraction increases gradually as the gas becomes optically thin due to the exponential decrease in density. However, only the uppermost 25% of the envelope is more than 80% ionized.

3.4 Discussion

We have derived a self consistent temperature grid for the envelope of 1 Del: see Figure 3.2. The average global temperature for this model is 5800±700 K (1σ): the density weighted is 5900±40 K (1σ). The difference between these 2 averages

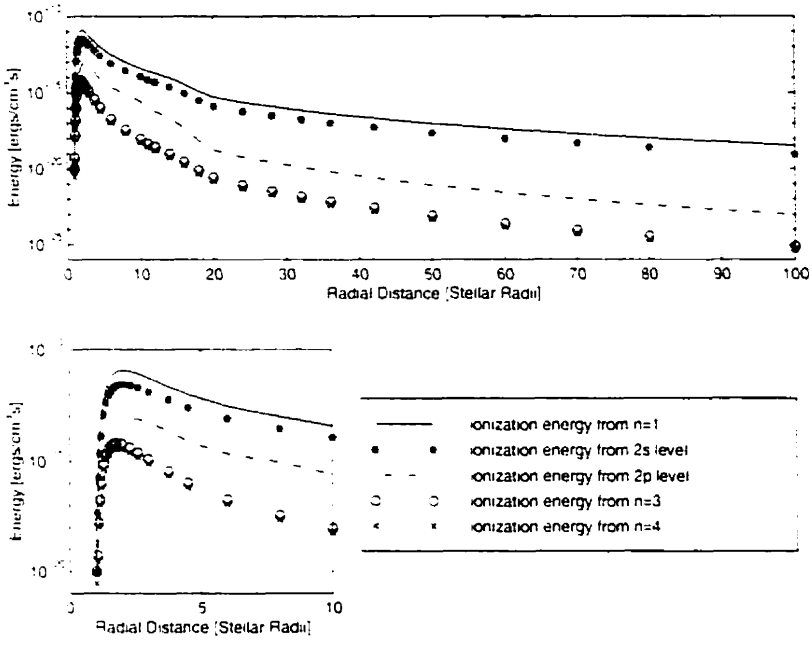

Figure 3.6: The same as Figure 3.5 for the upper envelope (J=19).

simply means that the temperature is slightly greater near the equatorial plane where the density is higher. These calculated values of temperature are considerably smaller than the isothermal temperature of 10,000 K assumed by MC.

Diffuse radiation produced within the envelope is not considered in this model: all of the ionizing radiation comes from the central star. Therefore, these calculated envelope temperatures based on equal energy gain and loss rates represent a lower limit. Since we were able to reproduce the gross features of the H_α line using the envelope temperatures calculated by this model, it is clear that there is sufficient stellar radiation present to ionize the circumstellar envelope and produce the relative line strength without any additional source of heating. Apparao and Tarafdar (1987, 1997a, 1997b) have reached the opposite conclusion. Their 1D model assumes the physical conditions at just one position in the circumstellar gas, and that the gas is completely ionized and ionization bound. No optical depth effects are included in H_α and they assume a kinetic temperature of 10^4 K. In constrast, the model calculations of the current investigation of 1 Del include both optical depth effects in the hydrogen lines and enforce radiative equilibrium, a critical ingredient

for modeling such strong lines. These effects are also discussed by van Kerkwijk, Waters, and Marlborough (1995). Finally, we note that observed fluxes that Apparao & Tarafdar fail to reproduce are the *highest values* observed for each Be spectral type.

The parameter ω' greatly affects the distribution of gas perpendicular to the equatorial plane. This, in turn, results in changes to the temperature distribution. In particular, larger values of ω' result in a much slower decrease in density perpendicular to the equatorial plane. As a consequence collisional terms are more effective in increasing the populations of upper levels from which photoionization can occur. Hence, the temperature does not drop off for regions near the uppermost edge of the envelope for larger values of ω'. Also, for larger values of ω' the surface density assumed must be reduced in order to reproduce the gross features of the Hα line. In addition, for larger values of ω' more of the line is formed further from the star where rotational velocities are reduced. This is evident from the shape of the line; with increasing values of ω' the width of the absorption component decreases. Therefore, the line width can be used as a tool to investigate at what radial distance from the star the line is formed.

In order to reproduce the gross features of the Hα line we had to assume that the envelope rotation was completely Keplerian so that the velocity did not decrease too fast with increasing distance from the star. Only then was the predicted model line sufficiently wide.

The temperature along the upper edge of the envelope is quite sensitive to minor changes in the model. The energy terms are all very small in magnitude because of the exponential decrease in density. Any small change in model parameters, which influences the level populations, affects the relative value of energy terms. This, in turn, modifies the temperature since it is calculated from the assumption of equal energy gain and loss rates. For example, changing the spacing of the grid locations in the radial direction has no significant effect on the calculated temperatures in the envelope except along the uppermost edge. Therefore, along the uppermost edge the quoted temperatures must be viewed as estimates. However,

since these regions have relatively small densities and since generally the emission goes as the number density squared. the uppermost region does not contribute to the observed emission lines in the optical portion of the spectrum.

Bibliography

Apparao, K. M. V. & Tarafdar, S. P., 1987. *ApJ* **322**, 976.

Apparao, K. M. V. & Tarafdar, S. P., 1997a. *J. Astrophys. Astr.* **18**, 145.

Apparao, K. M. V. & Tarafdar, S. P., 1997b. *Bull. Astr. Soc. India* **25**, 345.

Ashok, N. M., Bhatt, H. C., Kulkarni, P. V., & Joshi, S. C., 1984. *MNRAS* **211**, 471.

Balona, L. A., Henrichs, H. F., & Contel, J. M. L. (Eds.), 1994. *IAU Symp. 162, Pulsation, Rotation and Mass Loss in Early-Type Stars*. Dordrecht: Reidel.

Dougherty, S. M. & Taylor, A. R., 1992. *Nature* **359**, 808.

Marlborough, J. M., 1969. *ApJ* **156**, 135.

Marlborough, J. M. & Cowley, A. P., 1974. *ApJ* **187**, 99. (MC).

Millar, C. E. & Marlborough, J. M., 1998. *ApJ* **494**, 715. (MM).

Poeckert, R. & Marlborough, J. M., 1978. *ApJ* **220**, 940. (PM).

Quirrenbach, A., Hummel, C. A., Buscher, D. F., Armstrong, J. T., Mozurkewich, D., & II, N. M. E., 1993. *ApJ* **416**, L25.

Slettebak, A. & Carpenter, K. G., 1983. *ApJS* **53**, 869.

Slettebak, A. & Snow, T. P. (Eds.), 1987. *IAU Symp. 92, Physics of Be Stars*. Cambridge: Cambridge University Press.

Stee, P., de Araújo, F. X., Vakili, F., Mourard, D., Arnold, L., Bonneau, D., Morand, F., & Tallon-Bosc, I., 1995. *A&A* **300**, 219.

van Kerkwijk, M. H., Waters, L. B. F. M., & Marlborough, J. M., 1995. *A&A* **300**, 259.

Chapter 4

Diffuse Radiation[3]

4.1 Introduction

We have determined an upper limit to the kinetic temperature of the gas in the circumstellar envelopes of 2 Be stars, a hot star γ Cas, and a cooler star 1 Del, by including in an approximate manner the diffuse radiation produced in the envelope. We computed the temperature as a function of position by balancing at each position the rates of energy gain and energy loss. Photoionization, collisional de-excitation of bound levels and free-free absorption were assumed to contribute to the rate of energy gain; radiative recombination, collisional excitation and free-free emission contribute to the rate of energy loss. The kinetic temperature at a particular location is obtained from the requirement that the rates of energy gain and energy loss there are equal. These results, combined with previous investigations, establish the range of temperatures expected in the circumstellar envelopes of Be stars if the only source of energy input is the radiation field of the star.

The observed Balmer emission in Be stars is thought to arise from radiative recombination in ionized circumstellar material, concentrated toward both the equatorial plane and the star. These stars also have excess continuum radiation in the infrared and at longer wavelengths. In addition, Be stars have a high linear polarization which provides evidence for a non-spherical distribution of material. Recently the circumstellar envelopes of several

[3]A version of this chapter has been published: Millar C. E., Marlborough J. M., (1999) Rates of energy gain and loss in the circumstellar envelopes of Be stars: diffuse radiation, ApJ, 516, 276.

Be stars have been resolved, providing support for this view of a Be star: Dougherty and Taylor (1992), Quirrenbach et al. (1993), and Stee et al. (1995).

The Poeckert and Marlborough model (1978), hereafter the PM model, is an ad hoc model originally used to model the B0 star γ Cas. Recently, we have used this model to investigate the temperature of the circumstellar envelopes of both γ Cas and 1 Del, see Millar and Marlborough (1998, 1999a), hereafter MM, and MMa, respectively. We assumed that the gas dynamical terms in the equation for the conservation of energy are sufficiently small so that at each location the rate of radiative energy gain should equal the rate of radiative energy loss if the correct kinetic temperature were known. Photoionization, collisional de-excitation, and free-free absorption were assumed to contribute to the rate of energy gain; radiative recombination, collisional excitation, and free-free emission contribute to the rate of energy loss. We can test the appropriateness of the temperatures assumed in previous investigations by calculating the ratio of the rate of energy gain to the rate of energy loss at various locations within the envelope. If the correct temperature were assumed, this ratio would be exactly 1. If not, we adjust the temperature, determine again the ionization-equilibrium and re-calculate the ratio of energy gain to loss, until the ratio equals 1 to within some prescribed value.

In our previous investigations, we did not include the diffuse radiation field. Hence the temperature predicted represents a lower limit. An accurate determination of the diffuse radiation requires an integration over 4π at each location in the envelope. Rather than do this we have, instead, chosen to approximate the effect of the diffuse radiation by assuming that every recombination to level $n = 1$ results in a subsequent photoionization locally. This approximation is commonly referred to as the on-the-spot approximation (Osterbrock 1974). The additional ionization adds energy to the gas and contributes to heating of the circumstellar material. This simplification allows an upper limit to the temperature to be calculated. By combining the results of this investigation with earlier temperature calculations, we have determined the range of temperatures self consistently for various locations within the envelopes of Be stars.

4.2 Results According to the on-the-spot approximation every recombination to level n = 1 produces an ionizing photon which is re-absorbed locally. Since the density in the PM model decreases exponentially with increasing distance perpendicular to the equatorial plane, the uppermost portions of the envelope have very low densities. Although the gas there would be essentially completely ionized, the low density implies a low recombination rate to n = 1. Secondly it is doubtful that diffuse radiation produced at a particular location in a low density gas would be re-absorbed locally. Hence the on-the-spot approximation may not a reasonable one for the uppermost locations in the envelope. Therefore, we compare our results with and without the on-the-spot approximation in the denser regions of the envelope only. Specifically, this includes the region of the envelope from the equatorial plane to a distance half way between the equatorial plane and the upper edge. This volume comprises approximately 99% of the circumstellar gas.

The variation of temperature with radial position in the equatorial plane, and at a distance half way between the equatorial plane and the upper edge, respectively, for the star γ Cas is shown in Figures 4.1 and 4.2. For comparison, these Figures show both the temperature of MM, and the temperature determined by the inclusion of the diffuse radiation field. Figures 4.3 and 4.4 are the equivalent plots for the star 1 Del. The temperature grid for 1 Del was determined previously by MMa. The stellar parameters used for γ Cas and 1 Del are the same as those used by MM and MMa, respectively.

Generally, the inclusion of the diffuse radiation field increases the temperature locally due to the energy gain by additional photoionization from level n = 1. The largest temperature increases occur in regions where the degrees of ionization are the greatest: the more ionizations, the larger the number of recombinations, so that more ionizing photons are produced. Therefore, the differences between the temperatures predicted by MM and MMa, and the temperatures obtained by inclusion of the diffuse radiation field increase with increasing distance perpendicular to the equatorial plane as the degree of ionization increases. In contrast, in the equatorial plane differences between the predicted temperatures by MM, MMa and those obtained by inclusion of the diffuse field are not as large.

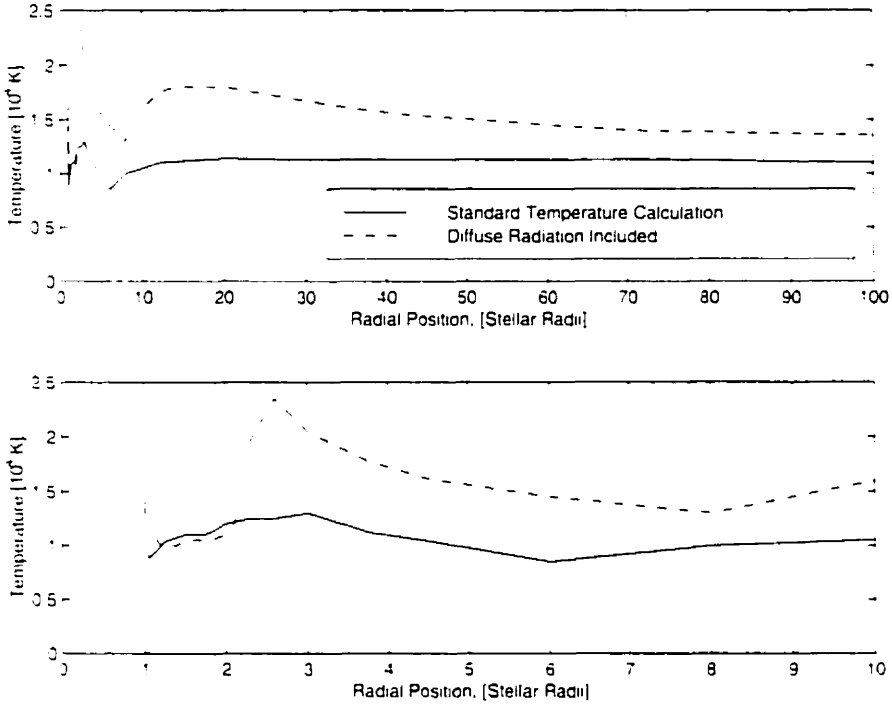

Figure 4.1: The temperature for which the energy gain balances the energy loss as a function of distance from the rotation axis in the equatorial plane for the star γ Cas. The predicted temperature determined by MM and the predicted temperature with the inclusion of the diffuse radiation field are shown for comparison. The lower portion of the figure is an enlargement of the region between 1 and 10 stellar radii.

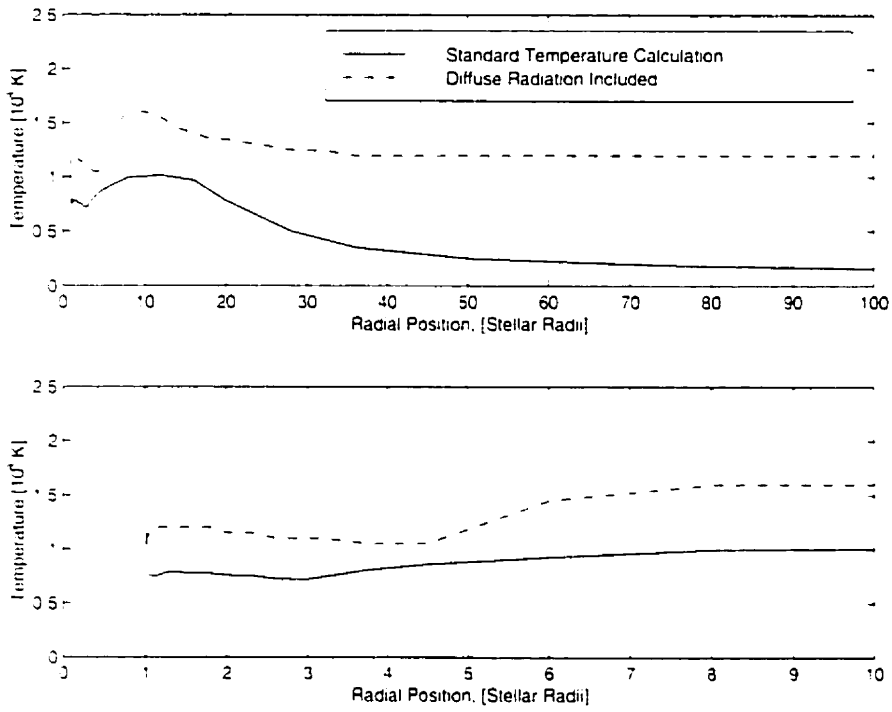

Figure 4.2: The temperature for which the energy gain balances the energy loss as a function of distance from the rotation axis at a location half way between the equatorial plane and the upper edge for the star γ Cas. The predicted temperature determined by MM and the predicted temperature with the inclusion of the diffuse radiation field are shown for comparison. The lower portion of the figure is an enlargement of the region between 1 and 10 stellar radii.

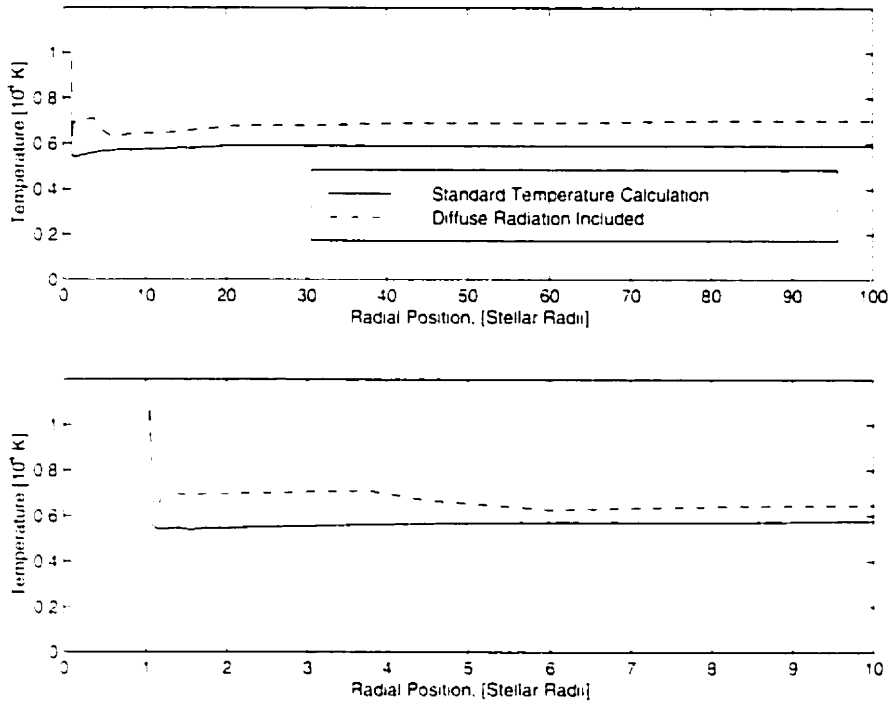

Figure 4.3: The same as Figure 4.1 for the star 1 Del.

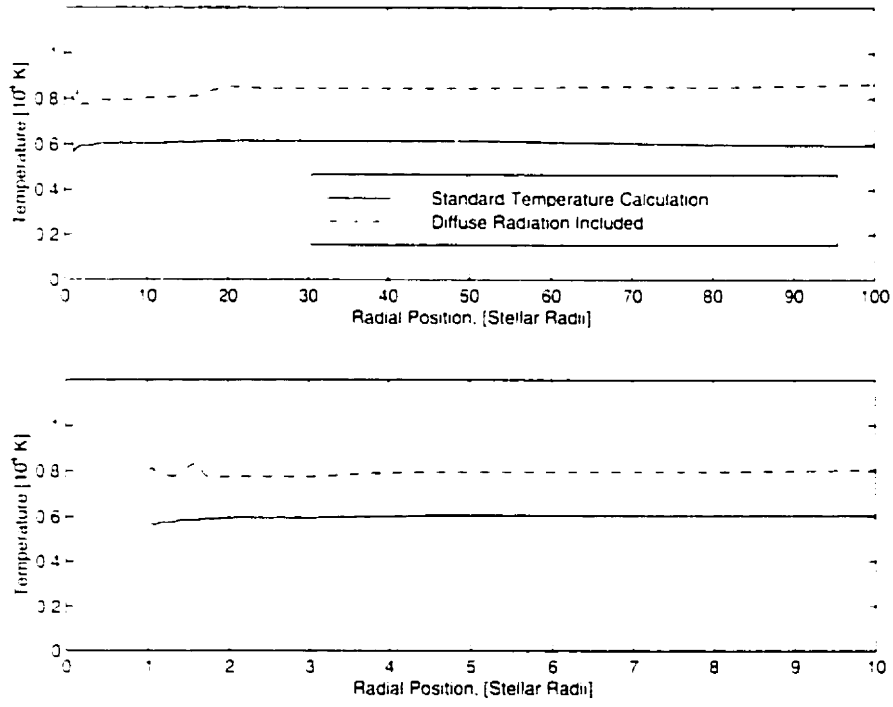

Figure 4.4: The same as Figure 4.2 for the star 1 Del.

In and near the equatorial plane where densities are the highest, the column densities in the ground state are large and the degree of ionization corresponding low. Consequently, the diffuse radiation field has essentially no significant effect for distances between 1 and 2 stellar radii for the star γ Cas since the numbers of recombinations to level n = 1 are very low. This can readily be observed in Figure 4.1. In these locations the density of the gas is high, column densities are very large, and only a very few recombinations to level n = 1 occur. Therefore, inclusion of the diffuse radiation field has little effect because of the small number of recombinations to level n = 1. The average temperature of the envelope with the diffuse radiation included is compared with the previous investigations of MM and MMa in Table 4.1; the uncertainties are 1σ values.

Table 4.1: A comparison of envelope temperatures with and without diffuse radiation for both 1 Del and γ Cas

	global average [K]	global average including diffuse radiation [K]	density weighted average [K]	density weighted average including diffuse radiation [K]
γ Cas	12000±4000	14000±3000	10700±90	14500±80
1 Del	5800±1000	6900±1700	5900±40	7200±50

4.3 Discussion and Conclusion

Table 4.1 clearly demonstrates that the inclusion of the diffuse radiation field increases the average envelope temperature. The diffuse radiation field provides additional heating due to the increase in photoionization from level n = 1. This increases the ionization fraction which subsequently increases the number of recombinations, with the result that the emission lines also increase in strength. The increase in strength of the H_α line with the inclusion of the diffuse field is quite dramatic for both γ Cas and 1 Del. For example, in order to reproduce the observed line with the diffuse field included for 1 Del, the number density must be reduced by a factor of approximately

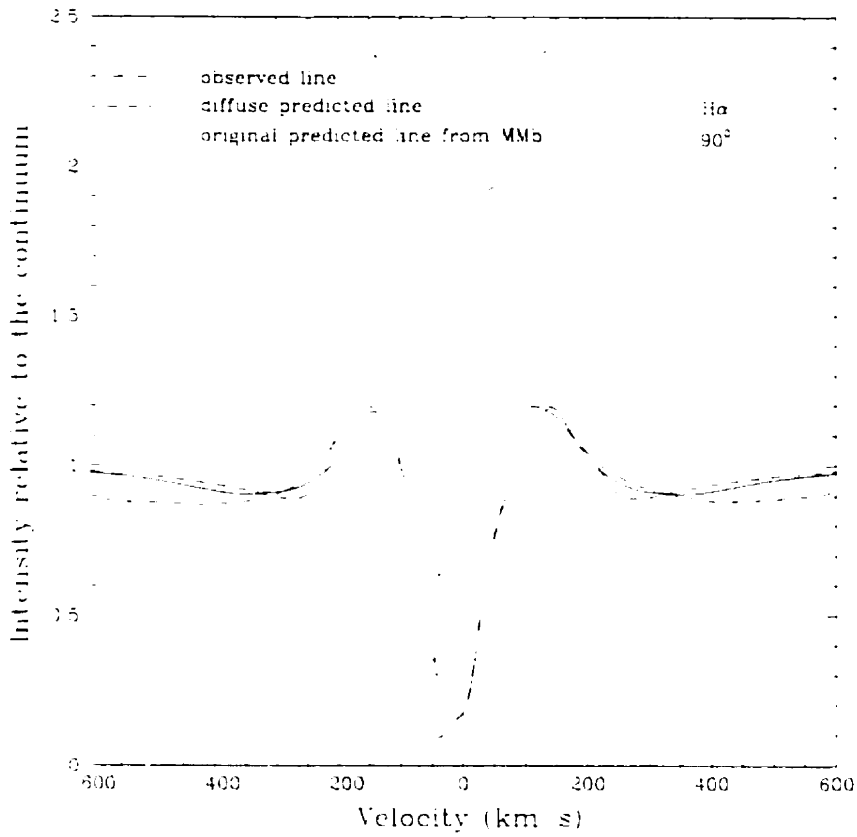

Figure 4.5: The predicted H_α line from MMa and the predicted line with the diffuse radiation field included for the star 1 Del. The models assume the disk is viewed edge on, that is, at an inclination angle of 90°. The observed line is also shown for comparison.

3, that is, from $4.2\text{x}10^{13}\,\text{cm}^{-3}$ to $1.3\text{x}10^{13}\,\text{cm}^{-3}$ at 4 stellar radii. The H_α line for 1Del from MMa, with the diffuse field included, is shown in Figure 4.5.

Since the diffuse radiation field increases the ionization fraction and subsequently increases the number of recombinations, the density must be reduced when the diffuse field is included in order to match the observed line. The reduction of assumed ρ_o also changes the derived temperatures: optical depths become smaller so that the stellar radiation can heat the gas more effectively. For 1 Del, there is a modest increase of the density weighted average temperature and a reduction in the simple global average temperature corresponding to the decrease in ρ_o. The reduction in ρ_o reduces the optical depths and allows more stellar

radiation to penetrate the envelope and heat the gas. This effect is most important in the densest regions of the envelope near the equatorial plane. The gas in the envelope of 1 Del is neutral in and near the equatorial plane and the effect of lowering the density increases the ionization fraction. Therefore, the density weighted average temperature increases slightly. In the upper regions of the envelope the gas is ionized; lowering the density in these regions simply reduces the amount of material that can be photoionized. This is the reason why the global average temperature decreases slightly for 1 Del with a reduction in ρ_o. The changes in temperature for 1 Del with the reduction in assumed ρ_o are modest and are, in fact, less than the estimated errors. The H_α line from MMa and that for the line predicted with lower ρ_o and inclusion of the diffuse radiation field are shown in Figure 4.6.

In order to reproduce the approximate amount of emission in the H_α line similar to the observed profile for γ Cas. (see PM), with the diffuse radiation field included, the assumed density at the surface of the star in the equatorial plane must be reduced by a factor of approximately 2.5. This reduction of ρ_o results in a modest decrease of approximately 1000 K in the derived temperature for both the density weighted temperature average and the simple global temperature for γ Cas. The global average is 13000 K $\pm$ 1700 K and the density weighted average is 12900 K $\pm$ 80 K. The envelope of γ Cas at the original density is almost completely ionized with the diffuse field included. The reduction in the density by decreasing the assumed value of ρ_o simply reduces the amount of gas that can be ionized and heated.

Our investigation has demonstrated that the inclusion of the diffuse radiation field is necessary in order to predict accurate kinetic temperatures for the circumstellar envelopes of Be stars. The on-the-spot approximation is a reasonable one to use to investigate the effect of the diffuse radiation field. It is not, however, a reasonable approximation for locations in the envelope where densities are very low since it is unlikely that diffuse radiation would be re-absorbed locally. In regions of low density, it is more likely that any ionizing radiation produced would be re-absorbed somewhere else in the envelope. However, since

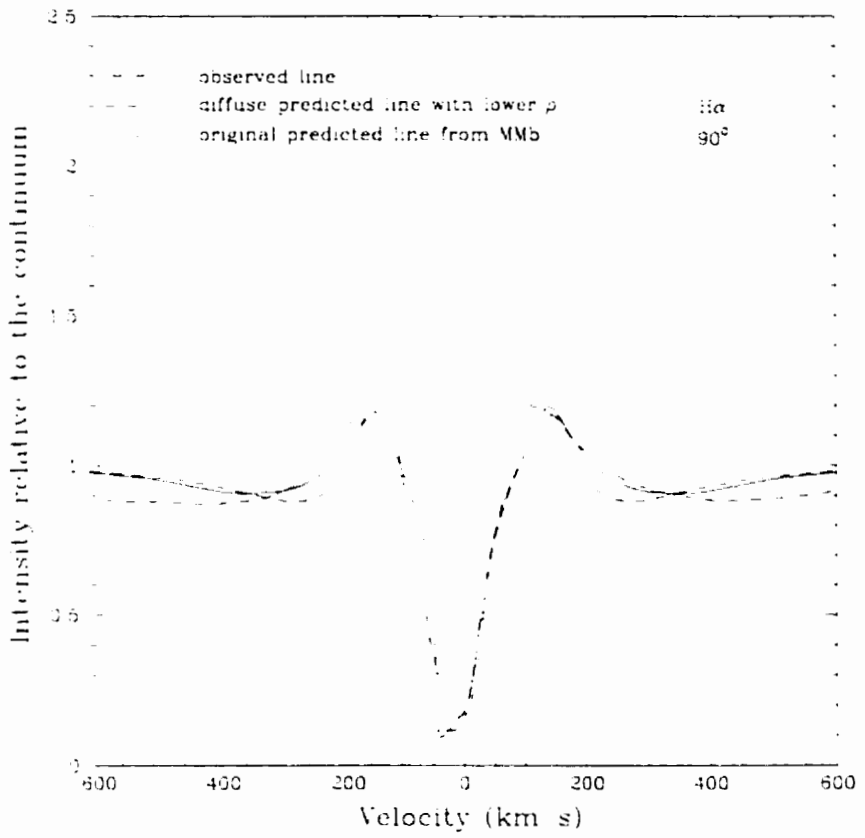

Figure 4.6: The predicted H_α line from MMa and the predicted line with the diffuse radiation field included with a lower ρ_o for the star 1 Del. The models assume the disk is viewed edge on, that is, at an inclination angle of 90°. The observed line is also shown for comparison.

recombination line strengths are proportional to the electron density squared. regions of low density do not contribute greatly to the observed lines.

Bibliography

Dougherty, S. M. & Taylor, A. R., 1992. *Nature* **359**, 808.

Millar, C. E. & Marlborough, J. M., 1998. *ApJ* **494**, 715. (MM).

Millar, C. E. & Marlborough, J. M., 1999. *ApJ* **516**, 280. (MMa).

Osterbrock, D. E., 1974. *Astrophysics of Gaseous Nebulae*. U.S.A.: W.H. Freeman and Company.

Poeckert, R. & Marlborough, J. M., 1978. *ApJ* **220**, 940. (PM).

Quirrenbach, A., Hummel, C. A., Buscher, D. F., Armstrong, J. T., Mozurkewich, D., & H. N. M. E., 1993. *ApJ* **416**, L25.

Stee, P., de Araújo, F. X., Vakili, F., Mourard, D., Arnold, L., Bonneau, D., Morand, F., & Tallon-Bosc, I., 1995. *A&A* **300**, 219.

Chapter 5

The Disk Model[4]

5.1 Introduction

We have investigated the kinetic temperatures assumed by Waters et al. (1987) for the circumstellar envelopes of a group of Be stars. Waters (1986a) introduced a simple equatorial disk model with $\rho(r) \propto r^{-n}$ to describe the physical characteristics of Be star disks. Since this equatorial disk model was applied to a large number of stars, it is important to ensure that the kinetic temperatures assumed by Waters et al. were reasonable. We have investigated their choice of kinetic temperature in two ways. Initially we tested the appropriateness of the temperatures assumed by evaluating the rates of energy gain and loss. Then, based on equating the local rates of energy gain and loss, we determined self-consistently the temperature structure for these envelopes. Our investigation included the following stars: γ Cas, δ Cen, ψ Per, and β CMi. For each of the stars examined we concluded that the constant temperature of the envelope assumed by Waters et al. was too high by a factor of 2 to 3.

It is thought that Be stars are characterized by a two component wind. The UV absorption lines are asymmetric with extended short wavelength wings, suggesting a low density, high velocity (500 to 3000 km s^{-1}), radiatively driven wind that is approximately spherical (Zaal et al. 1997). Emission lines in the optical and infrared are formed in a disk-like, higher density wind with an outflow velocity of less than 100 km s^{-1} (Waters and Marlborough 1992). It is only this portion of the wind that is considered in this thesis.

[4]A version of this chapter has been published: Millar C. E., Marlborough J. M., (1999) Rates of energy gain and loss in the circumstellar envelopes of Be stars: the disk model, ApJ, 526, 400.

A simple wedge-shaped, disk model was introduced by Waters (1986a) to describe the disk-like, equatorially concentrated wind. The density distribution is assumed to be given by the expression

$$\rho(r) = \rho_0 \{r/R_*\}^{-n}. \tag{5.1}$$

where ρ is the density, r is the radial distance, R_* is the stellar radius, ρ_0 is the density at $r = R_*$, and n is a number typically between 2 and 3.5. The density remains constant from the equatorial plane to the upper edge of the envelope on arcs of constant radial distance from the star. The outflow velocity is given by

$$v(r) = v_0 \{r/R_*\}^{n-2}. \tag{5.2}$$

where v is velocity at r and v_0 is velocity at R_*. The value of v_0 was assumed to be 5 km s^{-1} (Waters 1986a).

This model has the advantage that it is described by relatively few free parameters. In addition to ρ_0, v_0, and n, the other parameters that must be specified are the inclination angle i of the rotation axis with respect to the observer's direction, the outer radius of the disk, R_{disk}, and the opening angle, Θ, of the disk. It is assumed that no material lies above the *upper edge* of the envelope, which is defined as the boundary of the envelope that is at a maximum perpendicular distance from the equatorial plane as determined by the opening angle Θ.

In addition, and most important to this work, the kinetic temperature of the wind is a free parameter. The temperature determines the free-free and bound-free opacities and emissivities needed to interpret the IR excesses used in the curve of growth method to determine the wind parameters (Waters et al. 1987). These models have been used to derive the density structure and mass loss rates for Be star disks using data from IRAS (Waters et al. 1987, Waters 1986b, Waters 1986a, Dougherty et al. 1994). Waters et al.

(1987) assumed $T_{wind} = 0.8T_{eff}$. It is important to check the envelope temperatures assumed in order to assess the appropriateness of the disk model. In addition, matching the hydrogen profiles, such as H_α, provides important constraints on the wind parameters. A self-consistent temperature at each position in the envelope is necessary to predict accurate line profiles (Millar and Marlborough 1999a & 1999b).

In order to test the relevance of the wind temperatures assumed by Waters et al. (1987) we have calculated, using the identical wind parameters of Waters, the rate of energy gain and energy loss throughout the envelope and then, by balancing these rates, determined a self-consistent temperature at various positions in the envelope. We purposely chose the same parameters as Waters so that we could test the suitability of the constant temperatures assumed. Once the values of ρ_0, θ, and r_0 are assigned for a specific model, the mass loss rate is determined via the equation of continuity. Thus, the mass loss rates for our variable temperature models are the same as those determined by Waters et al. (1987).

We have examined the disk model for 4 Be stars which have a range in spectral type: γ Cas (B0IVe), δ Cen (B2IVne), ζ Per (B5Ve), and β CMi (B8Ve). We have tested the validity of the envelope temperature assumed by Waters et al. (1987) for each star and, more importantly, we have determined the variation of temperature throughout the envelope from the requirement of equal rates of radiative energy gain and radiative energy loss at each location.

5.2 Calculations

The rate of radiative energy gain and loss in the pure hydrogen gas was determined at various locations in the circumstellar envelope. At any position a unit volume of gas gains energy from photoionization, collisional de-excitation of excited levels and free-free absorption; it loses energy from recombination, collisional excitation and free-free emission. In a steady state, the kinetic temperature of the gas at a particular location is that temperature for which the rates of energy gain and loss are equal. Additional details may be found in Millar and Marlborough (1998).

We have calculated the ratio of energy gain to loss at various locations in the envelope using the same stellar parameters, including the isothermal envelope temperature assumed by Waters et al. (1987). If the kinetic temperature assumed by Waters et al. were correct, the energy ratios would equal unity everywhere in the envelope. A simple global average of this set of ratios provides a measure of how good or otherwise was the temperature assumed initially. A density weighted average of the energy ratio provides information about the assumed temperature in areas of the envelope where densities are high.

Subsequently, the program was modified to allow a temperature to be specified at each location considered in the envelope. For each star, the kinetic temperature assumed by Waters et al. (1987) was used as the initial guess at each location. The ionization-excitation program predicted the ratio of energy gain to loss for each grid location. Then the temperature at a particular location was adjusted, in steps of ± 500 K depending of the value of the ratio there. The program was then rerun using the modified temperature grid and the energy gain to loss ratios recalculated at each location. This iterative process was repeated until the ratio of gain to loss at each location considered was $1 \pm .02$. However, the individual temperatures are certainly not this accurate. The error in the level populations is approximately 5% due to the method by which they were calculated: this will result in errors in the temperature of approximately 10%.

5.3 Results

5.3.1 Isothermal Envelope Results The ratios of energy gain to energy loss for the isothermal envelope models assumed by Waters et al. (1987) are given in Table 5.1. For all of the stars investigated, the average of the ratio of energy gain to energy loss is less than one implying that the temperatures assumed by Waters were all too large. In order to achieve equal rates of gain and loss, the assumed wind temperatures must be reduced.

Table 5.1: Average envelope energy gain to loss ratios

HD	HR	Name	Spectral Type	T Wind [K]	Global Average of Ratios ($\pm 1\sigma$)	Density Weighted Average of Ratios ($\pm 1\sigma$)
5394	193	γ Cas	B0IVe	25000	0.56±.38	0.598±.003
105435	4621	δ Cen	B2IVne	16000	0.30±.13	0.368±.002
22192	1087	ζ Per	B5Ve	12000	0.26±.09	0.304±.001
58715	2845	β CMi	B8Ve	10000	0.17±.05	0.174±.001

The results for both the simple global average ratio and the density weighted average ratio are very similar for each star. This simply reflects the fact that at a particular radial position the disk model has a density distribution which varies very slowly with increasing distance perpendicular to the equatorial plane. This is in contrast to the Poeckert and Marlborough model (1978), hereafter PM, in which the density distribution decreases exponentially perpendicular to the equatorial plane.

5.3.2 Results for a Variable Temperature Envelope The temperature was calculated at 480 predetermined locations within the envelope. Twenty four radial positions were chosen so that there are more grid points close to the star where the density is the highest. At each radial position, 20 grid points (called J values) perpendicular to the equatorial plane were considered. It is important to realize that the J values which correspond to the mid-position of the disk are not at a constant height above the equatorial plane, but instead are at an increasing distance from the equatorial plane, since the disk flares with increasing radial distance. A schematic diagram of the disk model is shown in Waters et al. (1987). The final set of temperatures for each star corresponding to equal rates of energy gain and loss as a function of radial distance from the star for 3 locations in the envelope, the equatorial plane, (J= 1), the upper edge, (J= 19), and mid-way between

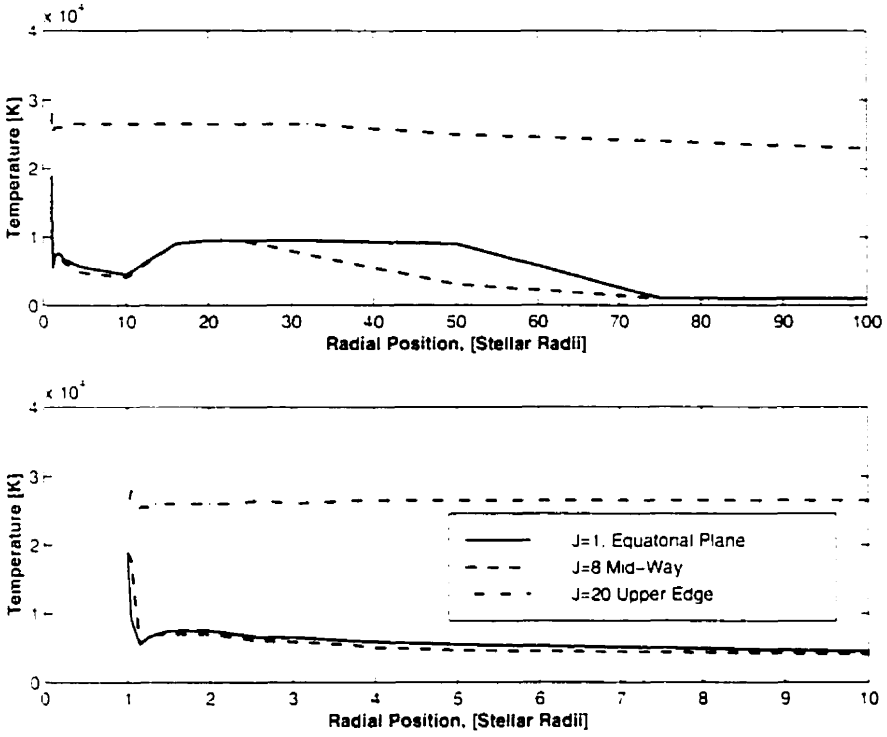

Figure 5.1: The temperature for which the energy gain balances the energy loss as a function of distance from the rotation axis for three locations in the circumstellar envelope: the equatorial plane (J=1), an intermediate location (J=6), and the upper edge (J = 20) for the star γ Cas.

the equatorial plane and upper edge, are displayed graphically in Figures 5.1, 5.2, 5.3, and 5.4 respectively. It is apparent from these figures that there are portions of the envelope where the temperature is approximately constant. However, there are differences in detail among the 4 stars investigated which are attributed to differences in the assumed ρ_0 and the effective temperature of the star.

Basically as a first order approximation, the temperature in the equatorial plane is fairly constant for all stars investigated. With increasing height above the equatorial plane, the temperature increases at locations where optical depths are not too large, generally at radial distances closer to the star; at larger radial distances the temperature may decrease due to both increasing optical depths and the geometrical dilution of stellar radiation. This effect is most pronounced for the coolest stars which have fewer ionizing continuum photons.

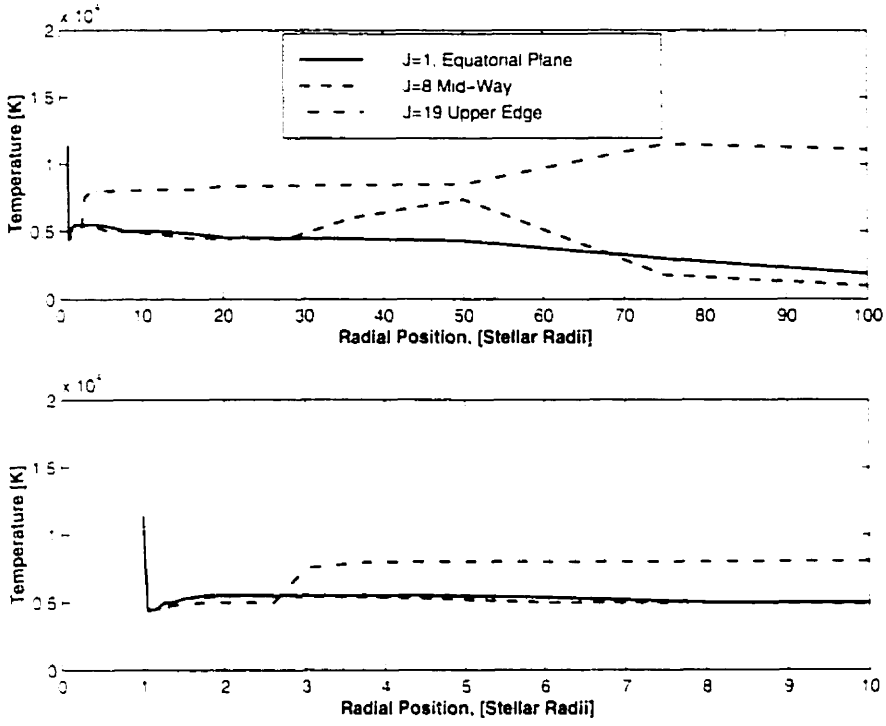

Figure 5.2: The same as Figure 5.1 for the star δ Cen.

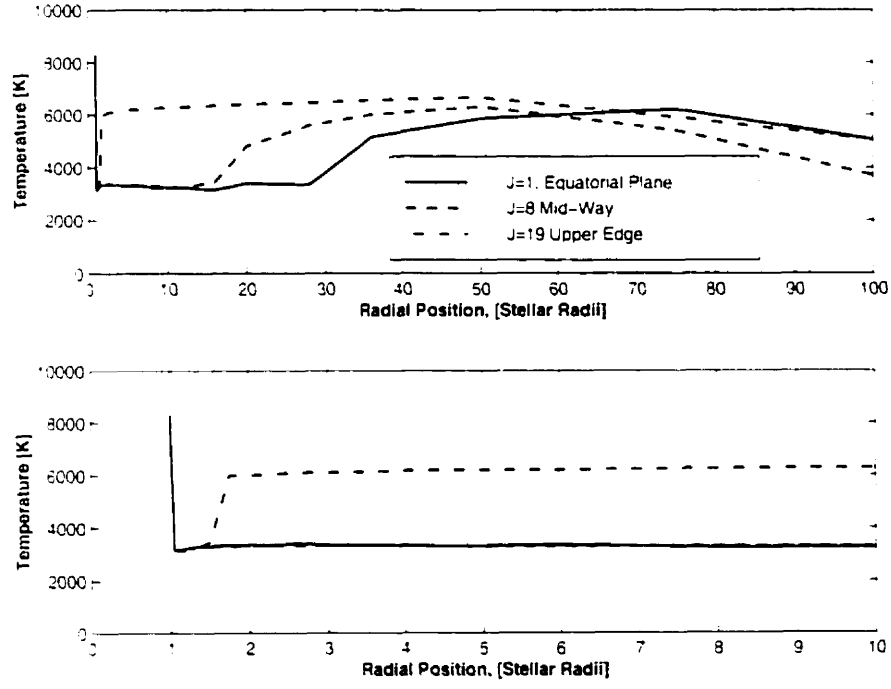

Figure 5.3: The same as Figure 5.1 for the star ϵ Per.

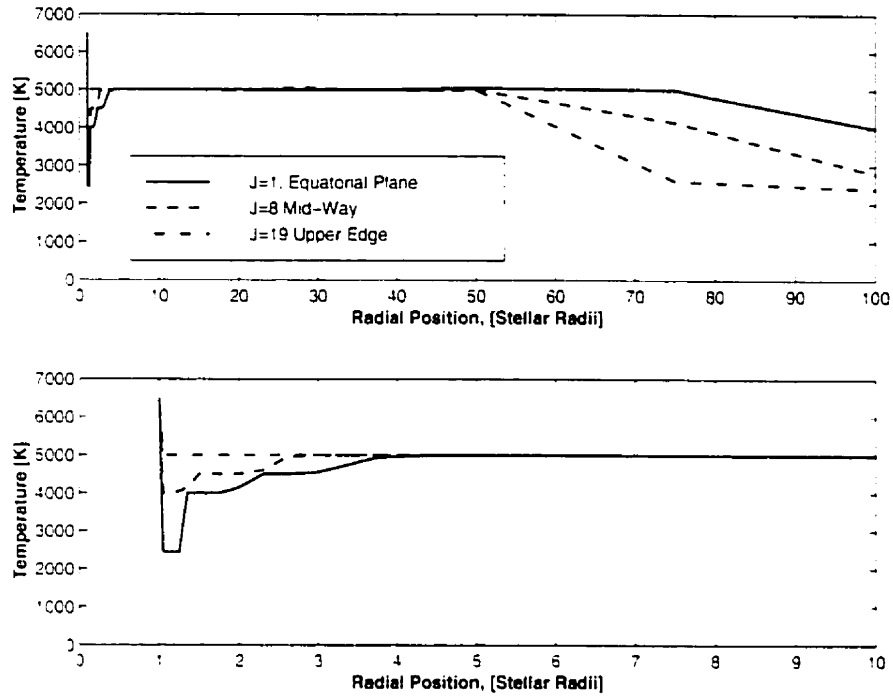

Figure 5.4: The same as Figure 5.1 for the star β CMi.

Eventually, since the lines of sight gradually traverse less material near the uppermost edge, the temperature steadily increases toward the upper edge of the envelope at all radial distances.

Generally, the upper edge is the hottest portion of the envelope. The exception is β CMi which, after some temperature variations near the star, has a constant temperature of approximately 5,000 K throughout the envelope out to a distance of 50 stellar radii; the temperature then drops by approximately 2,000 K along the upper edge. β CMi has an effective temperature of 12000 K (Waters et al. 1987). The other stars, γ Cas, δ Cen, and ζ Per have effective temperatures of 31000 K, 20000 K, and 15000K, respectively. If the effective temperature of β CMi were increased by a few thousand degrees K, then the upper edge of the envelope would become hotter than the interior under the condition of equal rates of energy gain and loss. For β CMi, the central star simply does not have enough ionizing photons to keep the outer edge hotter than the interior. Similarly for the B5 star, ζ Per, there is a slight decrease in temperature at large radial distances along the upper

edge: see Figure 5.3. However, this decrease is not as pronounced for ω Per as for β CMi, the coolest of the objects investigated.

The disc model has constant densities on arcs of constant radial distances from the star. Therefore, the density inside the envelope does not change significantly with increasing height above the equatorial plane. Consequently, the processes that are important in one part of the envelope are typically important elsewhere. As a result, although there are some temperature variations within the envelopes of the stars investigated and some differences between the stars investigated due to different effective temperatures and densities of the envelope, the temperatures within the envelope vary gradually. This is noticeably different from the PM model where the exponential decrease in density above the equatorial plane resulted in large temperature variations over relatively short distances within the envelope (Millar and Marlborough 1998). As a comparison, the density distribution along the equatorial plane in the disk model for γ Cas is approximately an order of magnitude *lower* than that assumed for the PM model. However, since the density falls off exponentially with increasing height above the equatorial plane in the PM model, the density for the disk model at the upper edge of the envelope, is approximately an order of magnitude *higher* than PM's density.

The outer edge of the envelope for γ Cas is quite hot due to the high effective temperature of the star. Adjacent to the uppermost edge, just inside the envelope there are differences in optical depths which result in temperature fluctuations due to rapidly changing conditions. These variations are unphysical and are due to large differences in optical depths along that part of the lines of sight considered between the assumed boundary of the upper edge, J = 20, and the next adjacent location considered, J = 19, in the z direction. Figure 5.1 shows the variation of the temperature with distance from the rotation axis for the J = 20 position. The model assumes that the envelope is optically thin in all lines along the upper edge, that is, at J = 20 and that there is no material beyond this assumed boundary. Therefore, this boundary is somewhat unphysical. Along the outer edge of the envelope, photons can escape freely into space. However, since the density remains constant along

lines of constant radial distance from the star and since γ Cas has the largest assumed ρ_0 of the stars investigated, the envelope at the J = 19 position is optically thick in all lines out to a radial distance of 2.75 stellar radii and optically thick in Lyman lines out to a radial distance of 20 stellar radii. Hence, between J = 20 and J = 19, conditions in the envelope change significantly. At a distance of 20 stellar radii the envelope becomes optically thin in all lines and a relatively constant temperature is maintained with increasing radial distance throughout the upper sections of the envelope.

5.3.3 Sources of Energy Gain and Loss Energy gain and loss are dominated by photoionization and radiative recombination at all locations of the envelope for all 4 stars investigated. Photoionization is the dominant source of energy gain to the gas for each star. Densities are never high enough for collisional energy terms to dominate. Nevertheless, collisional processes are important in populating upper energy levels from which electrons may then be ejected by photoionization. A radiative excitation of a bound electron followed by a collisional de-excitation represents a net energy gain to the gas. Conversely, a collisional excitation followed by a radiative de-excitation will result in an energy loss. Since the density is constant along radial arcs there is a modest reduction in density with increasing height perpendicular to the equatorial plane. As a result, collisional processes are somewhat more important in the equatorial plane than at the upper edge. Generally, for all 4 stars collisional energy gain (collisional de-excitation) is greater than collisional energy loss. For δ Cen and γ Cas, however, energy loss is greater than energy gain due to collisions at the upper edge of the envelope. These 2 stars have the higher effective temperatures. The collisional transition rate coefficient for the transition from level 1 to 2 for the model hydrogen atom considered and the collisional transitions allowed in this model are the most strongly affected by temperature. As a result, the higher kinetic temperatures due to the higher effective temperatures of these stars greatly increase this coefficient and consequently the total amount of collisional energy loss is increased.

For γ Cas, the main source of energy gain to the gas from photoionization in the equatorial plane comes from levels 2p and 2s out to a distance of approximately 65 stellar radii. At this distance from the star the photoionization energy from level 2p drops significantly. From this distance to the upper edge of the envelope, photoionization energy is dominated by levels 2s and n = 1. The number density of level 2p decreases due to the gradual decrease in total number density and the corresponding reduction in importance of collisional processes with the result that fewer electrons can get into the higher levels. Also, since level 2s is metastable, its number density builds up so that this level provides a larger proportion of the photoionization energy. Along the upper edge of the envelope, ionization from levels 1 and 2s contributes the most energy from the gas.

The dominate source of energy gain along the equatorial plane for the star δ Cen is photoionization from level 2p. Photoionization from levels 2s and $n = 3$ is also significant. Along the upper edge of the envelope, energy gain is dominated by photonization from 2p and 2s to a distance of approximately 60 stellar radii. At greater radial distances, energy gain is dominated by photoionization from level n = 1 along the upper edge.

The relative contributions to the energy gain by photoionization for ζ Per are the same as δ Cen both at the upper edge and in the equatorial plane. Along the upper edge, however, energy gain is dominated by photoionization from level n = 1 at radial distances greater than 65 stellar radii. The photoionization energy for β CMi comes from similar atomic levels as both δ Cen and ζ Per. However, along the equatorial plane, photoionization from level 3 only contributes out to a distance of approximately 3 stellar radii and then drops off rapidly in importance. This is due to a lower level population in level n = 3 which is a direct consequence of the lower density of the envelope of β CMi.

5.4 Conclusions

It is clear from Table 5.1 that the temperatures assumed by Waters et al. for the isothermal disks of these Be stars were too high. In order to obtain equal energy gain and loss rates it is necessary to lower the wind temperature. In a recent

parameter study of the disk model for the Be star ψ Per, the line shapes and ratios of line strengths were found to be strongly dependent on the temperature structure of the envelope (Marlborough, Zijlstra, and Waters 1997). Therefore, a self-consistent temperature distribution is an essential step to determine the physical parameters that describe conditions in the envelopes of Be stars. Figures 5.1, 5.2, 5.3, and 5.4 show the self-consistent temperature structure for the stars investigated. The differences in the temperature of the 4 stars with equal energy rates are due to differences in the assumed ρ_0 and in the effective temperatures of the stars. It is possible to determine a self-consistent set of temperatures which correspond to a given value of ρ_0 in order to match emission line shapes and ratios of the line strengths.

The envelope temperature distribution sets the continuum flux in the IR which may alter the value of the derived ρ_0 via the curve of growth method of Waters et al. (1987). The derived ρ_0 directly affects the hydrogen level populations as well as the model predictions of mass loss rates. Recall, the mass loss rates are set by the density and velocity distributions. However, the greatest uncertainty in the mass loss rates is due to the uncertainty in the assumed initial velocity, v_0. Unfortunately, the velocity distributions within Be star disks are not well known and an increase in v_0 will increase the mass loss rate.

The disk model has been used successfully to model the IR excess of Be stars. Dougherty et al. (1994) demonstrate the importance of the temperature distribution for emission line shapes and relative line strengths. Also, the temperature distribution in the envelope sets the ionization fraction. Knowledge of the ionization gradients within the envelope may prove to be a valuable probe of disk structure. Therefore, the approach used here, which determines the temperature self-consistently, is essential to decipher the characteristics of these disk-like envelopes. Self-consistent temperatures eliminate one additional degree of freedom in Be star models. The remaining parameters may then be determined with greater confidence.

Bibliography

Dougherty, S. M., Waters, L. B. F. M., Burki, G., Coté, J., Cramer, N., van Kerwijk, M. H., & Taylor, A. R., 1994, *A&A* **290**, 609.

Marlborough, J. M., Zijlstra, J. W., & Waters, L. B. F. M., 1997, *A&A* **321**, 867.

Millar, C. E. & Marlborough, J. M., 1998, *ApJ* **494**, 715, (MM).

Millar, C. E. & Marlborough, J. M., 1999a, *ApJ* **516**, 280, (MMa).

Millar, C. E. & Marlborough, J. M., 1999b, *ApJ* **516**, 276, (MMb).

Poeckert, R. & Marlborough, J. M., 1978, *ApJ* **220**, 940, (PM).

Waters, L. B. F. M., 1986a, *A&A* **162**, 121.

Waters, L. B. F. M., 1986b, *A&A* **159**, L1.

Waters, L. B. F. M., Coté, J., & Lamers, H. J. G. L. M., 1987, *A&A* **185**, 206.

Waters, L. B. F. M. & Marlborough, J. M., 1992, *A&A* **253**, L25.

Zaal, P. A., Waters, L. B. F. M., Geballe, T. R., & Marlborough, J. M., 1997, *A&A* **326**, 237.

Chapter 6

Energetics of Be Star Envelopes[5]

6.1 Introduction

We have calculated the total flux emitted in Hα, Pα, and Brα by the circumstellar envelope of both an early Be star, γ Cas, and a late Be star, 1 Del, assuming the central star is the only source of energy input into the circumstellar envelope. These estimates are based on the Be star models of Millar and Marlborough (1998, 1999a, 1999b) which have self-consistent temperature distributions determined by equating the local rates of energy gain and energy loss in the envelopes. We find that an additional source of ionizing photons, as argued by Apparao (1998), is not necessary to account for the observed emission.

The origin of the observed Balmer emission in Be stars is principally due to radiative recombination in a disk-like envelope of ionized circumstellar gas. Be stars can exhibit variations in emission on a wide range of time scales. The mechanism which creates and maintains these disks is not fully understood. Rapid rotation certainly contributes, but because rotation is typically only ~ 0.8 of the critical velocity, another mechanism must be functioning. Proposed models to explain the formation of these disks include, for example, the wind compressed disk model (Bjorkman and Cassinelli 1993), non-radial pulsations (Vogt and Penrod 1983), and non-spherical, radiatively-driven wind models (Puls, Petrenz, and Owocki 1999).

[5] A version of this chapter has been published: Millar C. E., Sigut T. A. A., & Marlborough J. M., (2000) Energetics of Be Star Envelopes: The Continuum Re-processing Efficiency of Be Star Circumstellar Disks, MNRAS, 312, 465.

The disk-like circumstellar gas is highly concentrated in the equatorial regions surrounding the star. Compared to a typical H II region, the disk-like envelope has larger densities, smaller geometrical dilution of stellar radiation, significant hydrogen photoionization from excited states, and supersonic macroscopic velocities. Typical values of temperature, outflow velocity, and number density in the envelope are 10^4 K, 10's of km s^{-1}, and 10^{12} cm^{-3}, respectively. Hence, many of the simplifying assumptions which apply to H II regions are invalid. As a consequence, ad hoc models have been developed for Be star envelopes by necessity, due to the complexity of the equations which describe the structure and dynamics of the circumstellar material. The Poeckert Marlborough model (1978), hereafter PM, is one such model which has been successful in describing some aspects of these disks for a range of Be stars. In the PM model an exponential density distribution perpendicular to the equatorial plane is assumed, and as a result, the gas is dense in and near the equatorial plane but decreases rapidly in density with increasing distance from the plane. Recent direct images of several Be stars (Quirrenbach et al. 1997) and spectropolarimetric results (Wood et al. 1997) demonstrate that Be star disks are indeed quite thin making the PM model attractive.

For most models of the past, it has been customary to assume either a constant temperature for the entire envelope or a simple temperature distribution with the temperature decreasing as a power law with increasing distance from the central star. In contrast to this, Millar and Marlborough (1998), hereafter MM, developed a method to determine the disk temperature self-consistently, thereby eliminating the need to assume an envelope temperature distribution. MM modified the PM code to calculate the energy gain and loss rates at positions in the gas. If the correct temperature were assumed at a particular position, the rate of energy gain there would equal the rate of energy loss. If not, the temperature was adjusted iteratively and atomic level populations re-calculated until the energy gain and loss rates were equal. The result of this procedure is a self-consistent set of temperatures for various positions throughout the envelope. See MM and Millar and Marlborough (1999b) for further details as applied to γ Cas, an early-type Be star (B0 IVe), and Millar and Marl-

borough (1999a & 1999b), for 1 Del, a late-type Be star (B8-9e). This work demonstrates that it is possible to reproduce relative line strengths, namely Hα, with a self-consistent temperature distribution.

However, Apparao and Tarafdar, hereafter AT, in a series of papers (1987, 1997a, 1997b), have argued that there is not sufficient stellar UV continuum radiation present in late type Be stars to ionize enough gas in order to produce the observed absolute fluxes. AT assume a model with a shell geometry, 10^{12} cm from the central star, and consider only radially outwardly and inwardly propagating rays. They also perform their calculation at only one position in the envelope having an assumed constant density, and they also *assume* a constant gas temperature of 10^4 K. AT also assume that the observed emission lines are formed by pure recombination, under case B conditions, in the ionized disk of the Be star. Recently, Apparao (1998) has reiterated the results of their work. We, along with Apparao (1998), note that there is in principle more than enough flux in the stellar continuum to account for the observed line emission; the debate is over re-processing efficiency. AT claim that the efficiency of Be star disks in converting stellar continuum photons into emission lines is simply not high enough for later spectral types. We disagree with this conclusion.

In this chapter, we evaluate the total flux escaping from our model Be envelopes, in contrast to that along a particular line of sight, in the important Hα, Pα, and Brα transitions. To do so, we estimated a local escape probability for line photons in each transition from each volume element in the circumstellar disk. This simple treatment is consistent with the inclusion of radiative line losses in the self-consistent temperature disk models of MM, and should be of sufficient accuracy to address the large deficiencies ($\sim 10^3$) claimed by AT for the late-type Be stars. This work represents the first time that the flux calculations have been obtained with models which have self-consistent temperatures determined throughout the circumstellar envelope. Others have calculated these fluxes, but in each case the envelope temperatures were assumed (Kastner and Mazzali 1989, Stee et al. 1995). Before presenting these flux estimates we will first discuss the role played by line optical depths.

6.2 Calculations: Hα, Pα, and Brα Line Fluxes

6.2.1 Pure Case B Recombination In their analysis, AT assume that the observed emission lines are formed by pure recombination, under case B conditions. If this assumption is correct, the total flux escaping in the $j \rightarrow i$ transition of hydrogen is given by

$$F(ji) = h\nu_{ji}\,\alpha_{ji}^{B} \int_{\rm Disk} N_e^2\, dV = h\nu_{ji}\,\alpha_{ji}^{B}\, EM_{\rm Disk}\,. \tag{6.1}$$

where h is Planck's constant, ν_{ji} is the line frequency, α_{ji}^{B} is the appropriate case B recombination coefficient, N_e is the number density of free electrons, and the integration is over the volume, which we, unlike AT, take to be a disk. Thus the line flux is proportional to the emission measure of the disk, $EM_{\rm Disk}$. The required atomic data and recombination coefficients for the three hydrogen transitions considered in this work (Hα, Pα, and Brα) are given in Table 6.1. The recombination coefficients adopted are for Te = 10^4 K and $\log(N_e) = 6$, the same conditions as adopted by AT, in order to compare directly to their computed fluxes.

Table 6.1: Atomic data and recombination coefficients.The α_{ji}^{B} recombination coefficients are for Te = 10^4 K and $N_e = 10^6\,{\rm cm}^{-3}$ and are adopted from Osterbrock (1989).

Transition	j	i	λ μm	A_{ji} s^{-1}	α_{ji}^{B} $cm^3 s^{-1}$
Hα.....	3	2	0.6563	4.470e+7	1.16e-13
Pα.....	4	3	1.8751	8.986e+6	3.75e-14
Brα.....	5	4	4.0512	2.699e+6	3.94e-14

In this approximation, the Hα flux, for example, is controlled only by $EM_{\rm Disk}$ and thus an estimate of N_e is required throughout the disk. AT include photoionization from hydrogen levels n= 1 and 2 and also approximately account for the thermalization of Lyα, as the latter is well known to significantly increase the n= 2 population, making Balmer photoionizations more important (for example see Kwan and Krolik 1981 in the case of

AGN). AT conclude that case B recombination fluxes do not reproduce the maximum Hα fluxes of Ashok et al. (1984) for Be stars later than $\sim$ B5. However, their calculation is performed at only one position in the envelope having an assumed constant density, and an assumed temperature.

In order to compare with AT as directly as possible, we have computed the hydrogen line fluxes using equation (6.1) for our models of γ Cas and 1 Del. This calculation includes all relevant atomic processes for a 5 level hydrogen atom, enforces radiative equilibrium, and uses the 2D disk geometry of PM. Fluxes from two models for each Be star are presented, one constructed with, and one without, the on-the-spot approximation for the diffuse radiation generated within the envelope (Osterbrock 1989). The diffuse radiation increases the degree of ionization due to increased photoionization from level n = 1. With the diffuse radiation included, the density required at the stellar surface to match the observed relative strength of Hα is approximately a factor of 3 lower for both γ Cas and 1 Del (Millar and Marlborough 1999b). Note that the density at the stellar surface fixes, by continuity, the density throughout the equatorial plane.

Figure 6.1 shows the derived temperatures for γ Cas using the parameters of PM and MM. Due to the exponential density distribution perpendicular to the equatorial plane and to the high equatorial densities, there are significant temperature variations both near the star and near the equatorial plane. These temperature variations lead to ionization gradients within the circumstellar envelope which may prove to be a valuable probe into the structure of these envelopes.

The hydrogen line fluxes of equation (6.1) are presented in column 3 of Table 6.2 for γ Cas and 1 Del, both of which have self-consistently determined envelope temperatures. In addition, unlike AT, a realistic disk geometry has been used. For comparison, typical observed values of the Hα luminosity range from approximately 10^{34}erg s^{-1} for early type Be stars to 10^{32}erg s^{-1} for late type Be stars (Ashok et al. 1984).

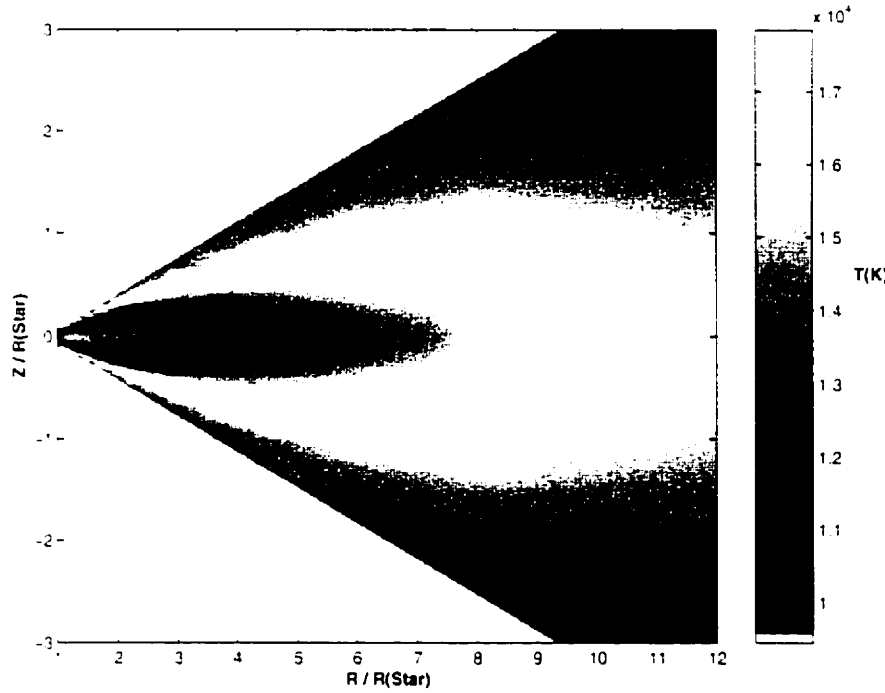

Figure 6.1: The temperature for which the local energy gain balances energy loss for the circumstellar disk of γ Cas as a function of distance from the rotation axis (R) and height above the equatorial plane (Z).

In the following sections, we shall demonstrate that many of the above assumptions are incorrect and that the emission line fluxes cannot be reliably computed with an expression such as equation (6.1). In addition to using the correct geometry of the emitting region (a disk), optical depth effects and other line formation mechanisms, such as collisional excitation, must be included. We now address these remaining important physical effects.

Table 6.2: Calculated hydrogen line fluxes. γ Cas is B0IVe star with a luminosity of $1.3\text{x}10^{38}$ erg s^{-1} and a radius of 10 solar radii. 1Del is a B8-9e shell star with a luminosity of $9.5\text{x}10^{35}$ erg s^{-1} and a radius of 3.3 solar radii.

Star	Diffuse Radiation	Eq.(6.1) [erg s^{-1}]	Eq.(6.2) [erg s^{-1}]	Eq.(6.3) [erg s^{-1}]
			Hα Flux	
γ Cas	yes	$8.3\text{x}10^{35}$	$2.1\text{x}10^{32}$	$5.9\text{x}10^{33}$
	no	$2.3\text{x}10^{36}$	$6.3\text{x}10^{31}$	$6.9\text{x}10^{33}$
1 Del	yes	$2.4\text{x}10^{34}$	$7.5\text{x}10^{28}$	$1.3\text{x}10^{32}$
	no	$3.1\text{x}10^{33}$	$4.9\text{x}10^{29}$	$2.3\text{x}10^{32}$
			Pα Flux	
γ Cas	yes	$8.1\text{x}10^{34}$	$1.5\text{x}10^{32}$	$2.5\text{x}10^{32}$
	no	$2.4\text{x}10^{35}$	$1.4\text{x}10^{32}$	$3.1\text{x}10^{32}$
1 Del	yes	$2.7\text{x}10^{33}$	$3.8\text{x}10^{31}$	$2.7\text{x}10^{31}$
	no	$3.5\text{x}10^{32}$	$6.6\text{x}10^{30}$	$5.8\text{x}10^{30}$
			Brα Flux	
γ Cas	yes	$4.1\text{x}10^{34}$	$1.4\text{x}10^{32}$	$1.4\text{x}10^{31}$
	no	$1.2\text{x}10^{35}$	$2.0\text{x}10^{32}$	$2.3\text{x}10^{31}$
1 Del	yes	$1.3\text{x}10^{33}$	$3.7\text{x}10^{31}$	$3.4\text{x}10^{30}$
	no	$1.7\text{x}10^{32}$	$1.1\text{x}10^{31}$	$1.3\text{x}10^{30}$

6.2.2 Inclusion of Line Optical Depths It is assumed in equation (6.1) and by AT that all photons generated by recombination escape. We have found, however, that for our models there are portions of the envelope both near the star and the equatorial plane that are optically thick in some or all of Hα, Pα, and Brα. Figure 6.2 shows the line centre optical depth from the equatorial plane to the upper edge of the envelope for each hydrogen

transition. Very large optical depths are predicted, particularly close to the star where the densities (and N_e - see figure insert) are large. From Figure 6.2 it is clear that the line fluxes cannot be given by equation (6.1) as not all the photons can escape.

As an ad hoc correction for this effect, we have computed the fluxes using

$$F(ji) = h\nu_{ji}\,\alpha^B_{ji}\int_{\rm Disk} P^{esc}_{ji}\,N_e^{\,2}\,dV\,. \tag{6.2}$$

where P^{esc}_{ji} is the fraction of photons which escape from the volume element. P^{esc}_{ji} is estimated based on the line center optical depth, τ_o, along a path perpendicular to the equatorial plane from the volume element to the upper edge of the envelope. See MM or Marlborough (1969) for additional details: P^{esc}_{ji} corresponds to the cases to which these papers refer. Typically, for large τ_o, $P^{esc} \propto \tau_o^{-1}$ and thus the optical depth corrections to the escaping flux are very large. Column 4 of Table 6.1 contains results based on equation (6.2). Large changes in the hydrogen line fluxes are apparent with reductions in the Hα fluxes to levels far below observation. Two conclusions follow: (i) it is imperative to account for the optical depths and (ii) case B recombination is not an accurate approximation.

6.2.3 Escape Probability Fluxes Equation (6.2) is still not correct, however, as the hydrogen ionization balance is not correctly given by case B recombination due to the optical depth effects previously mentioned. A proper estimate of the hydrogen line fluxes includes both collisional excitation and optical depth effects, and can be obtained by using the standard escape probability approximation for the flux divergence.

$$F(ji) = h\nu_{ji}\,A_{ji}\int_{\rm Disk} N_j\,P^{esc}_{ji}\,dV\,. \tag{6.3}$$

where N_j is the number density of level n = j and A_{ji} is the spontaneous radiative transition probability (see Table 6.1). The results of this calculation are displayed in column 5 of Table 6.2. Note the large increase over equation (6.2), even with the P^{esc}_{ji} factor, to values which roughly agree with the observations of Ashok et al. (1984).

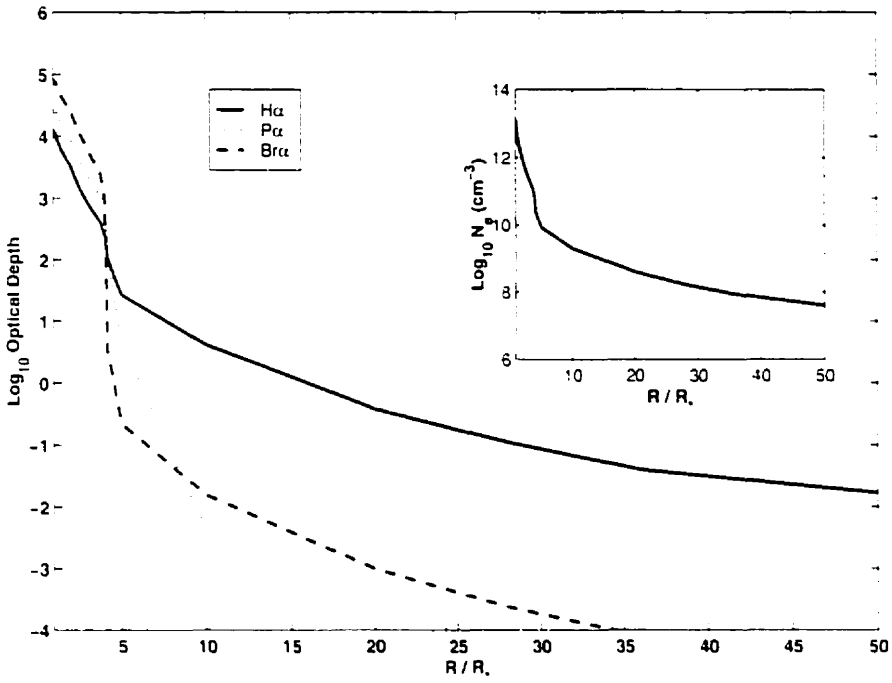

Figure 6.2: The log of the line centre optical depth, τ_o, for the indicated hydrogen transitions from the equatorial plane to the upper edge of the circumstellar disk for γ Cas as a function of distance from the rotation axis (R). Shown in the insert is the log of electron density in the equatorial plane.

The Hα fluxes from 1 Del deserve comment. Both the diffuse and non-diffuse models match, by construction, the relative Hα line profile for 1 Del with the disk assumed to be seen edge on (Millar and Marlborough 1999a&b). However, the models predict different fluxes for other viewing angles and our current estimates for the *total flux* emitted from the entire envelope in Hα differ by a factor of ~2.

6.3 Discussion

As previously noted, typical observed values of Hα luminosities range from approximately $10^{34}\mathrm{erg\,s^{-1}}$ for early type Be stars to $10^{32}\mathrm{erg\,s^{-1}}$ for late type Be stars (Ashok et al. 1984, Kastner and Mazzali 1989). Comparing to the fluxes listed in Table 6.2 which represent the total energy losses in these lines from the circumstellar envelope, we see that our best estimates for $F(\mathrm{H}\alpha)$, those computed with equation (6.3),

are in good agreement with these observations for both early and late-type Be Stars. For the late-type Be stars, we are in disagreement with the theoretical flux estimates of AT who give $\sim 2 \times 10^{29}$ erg s^{-1} as their best estimate for $\sim$ B8e. The discrepancy is even larger if one compares with our flux estimate based on equation (6.1), a result which by construction, should be most comparable to AT. However, this flux estimate is a large overestimate of typically observed fluxes, and the inclusion of collisional excitation and optical depth effects are critically important to the formation of the Hα line.

One caveat in comparing our computed Hα fluxes with observations is that the observed absolute fluxes are obtained from measured Hα equivalent widths, $EW_{\rm H\alpha}$, for a particular (sometimes unknown) line of sight and are converted to absolute fluxes via

$$F(\mathrm{H}\alpha) \approx 4\pi R_*^2 \, B_{\rm H\alpha}(T_*) \, EW_{\rm H\alpha}. \tag{6.4}$$

This conversion depends upon accurate radii, R_*, and continuum fluxes for the underlying stellar photospheres. Also, accurately known distances are required to convert observed fluxes to absolute fluxes. In equation (6.4), the continuum photospheric flux, $B_{\rm H\alpha}$, is approximated by the Planck function at the wavelength of Hα for $T_* \approx T_{eff}$, as done by Ashok et al. (1984). In addition, equation (6.4) assumes that the stellar photosphere alone contributes to the continuum flux at Hα, an assumption which has been criticized by Stee et al. (1995) whose models indicate 10-20% contributions of the disk envelope to the continuum emission of Hα. Thus, there are large uncertainties involved in the transition from routinely observed equivalent width measurements to absolute line fluxes. Stee et al. (1998) and Kastner and Mazzali (1989) give values of the Hα luminosity for γ Cas of 6.36 x 10^{34} and 3.24 x 10^{34} erg s^{-1}, respectively with the difference in the values discussed by Stee et al.

The characteristic size of the Hα emitting region can now be constrained directly by interferometric observations which resolve the circumstellar disks of nearby Be Stars (Quirrenbach et al.1994, 1997; Stee et al. 1995). In Figure 6.3, we plot the radial integrand, dF/dR, corresponding to equation (6.3) for the Hα fluxes of γ Cas and 1 Del. In the case

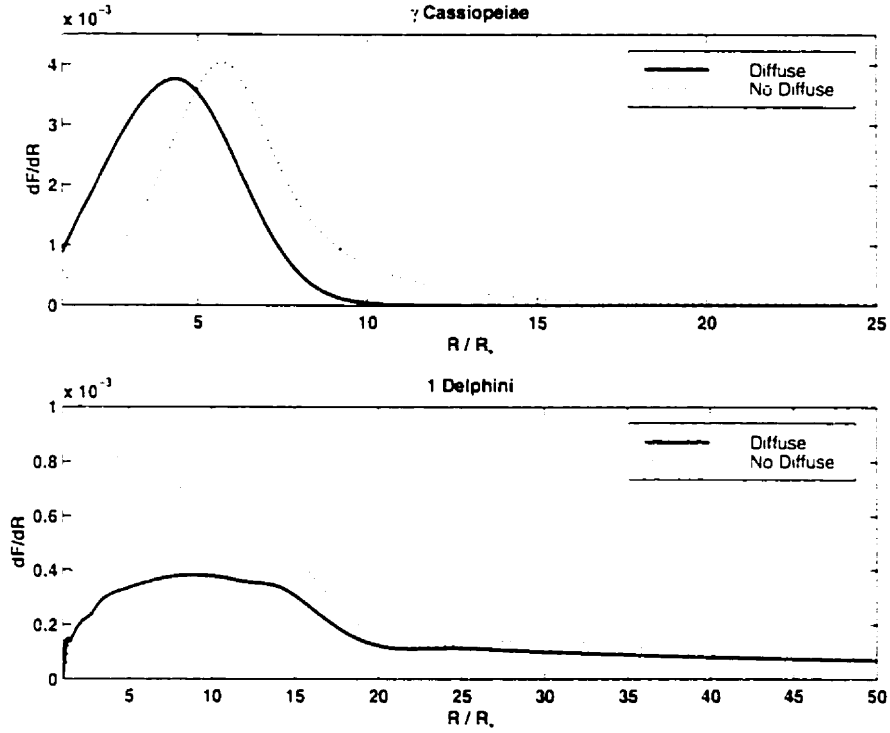

Figure 6.3: The radial derivative of the escape probability flux (equation 6.3) for γ Cas (upper panel) and 1 Del (lower panel) for models including (solid lines) and excluding (dotted lines) the diffuse component of the photoionizing radiation field. The area under each curve is the total flux escaping the envelope in Hα divided by R_*^3. The units of dF/dR are ergs cm^{-3} s^{-1}.

of γ Cas, we see a maximal contribution at about 5 stellar radii. Quirrenbach et al. (1997) obtain $\sim$ 6 stellar radii as the FWHM of the Hα emitting region as based on Gaussian fits to observed visibilities as obtained by interferometric observations. The predicted contributions from 1 Del are much broader, giving significant contributions out to 10–15 stellar radii. There are no observations to compare with our models for 1 Del, although this radial extent does seem larger than expected on the basis of 1 Del's spectral type (see Quirrenbach et al. 1997, Figure 8).

Comparing our results in Table 6.2 with these observations, we find no clear case for an additional source of ionizing radiation in order to produce the observed Hα emission for our particular choice of model parameters for either γ Cas or 1 Del. The discrepancies between Apparao's work and our calculations are due mainly to our realistic 2D geometry, and the

inclusion of collisional excitation and optical depths in Hα. That case B recombination is inappropriate for the calculation of hydrogen line fluxes from Be envelopes has also been discussed by Hony et al. (2000). The importance of optical depths for line emission in Be stars is also discussed by van Kerkwijk et al. (1995).

Commensurate with these observational uncertainties are theoretical uncertainties in the calculation of the line fluxes. The escape probability approximation has been used, with each volume element assigned an escape probability based solely on the optical depth to the upper edge of the disk, along a ray perpendicular to the equatorial plane; this approximation is consistent with the treatment of radiative line losses in the underlying models. The enhancement of the escape probabilities due to the Doppler shifting of material by the macroscopic velocity field of the disk has been ignored, although inclusion of this effect on the line fluxes and the disk model itself would certainly be worthwhile. Nevertheless, we do not expect that these uncertainties will affect the basic conclusions of this work that the UV energy input of the underlying star is more than sufficient to explain the observed Hα fluxes, as opposed to failing to do so by several orders of magnitude as suggested by AT.

6.4 Conclusions

We have computed hydrogen line fluxes emitted in the important Hα, Pα, and Brα transitions by the circumstellar envelopes of early-type and late-type Be stars. These lines fluxes are based on models with self-consistent envelope temperatures which balance local energy loss and gain and which, individually, match the relative Hα line profiles of γ Cas and 1 Del. Using these models as typical of Be stars of their respective spectral types, we find that we can also successfully match the absolute Hα line fluxes of Ashok et al. (1984) for both early and late-type Be Stars. Our results are in disagreement with the suggestion of AT that an additional source of UV photoionizing radiation is required to explain the absolute Hα line fluxes from late-type Be stars. We find to the contrary that there is no clear case for an additional source of ionizing radiation. The observed Hα fluxes

are consistent with the underlying stellar photosphere as the only source of photoionization energy input into the circumstellar disks.

Bibliography

Apparao, K. M. V., 1998. *Be Star Newsletter* **33**.

Apparao, K. M. V. & Tarafdar, S. P., 1987. *ApJ* **322**, 976.

Apparao, K. M. V. & Tarafdar, S. P., 1997a. *J. Astrophys. Astr.* **18**, 145.

Apparao, K. M. V. & Tarafdar, S. P., 1997b. *Bull. Astr. Soc. India* **25**, 345.

Ashok, N. M., Bhatt, H. C., Kulkarni, P. V., & Joshi, S. C., 1984. *MNRAS* **211**, 471.

Bjorkman, J. E. & Cassinelli, J. P., 1993. *ApJ* **409**, 429.

Hony, S., Waters, L. B. F. M., Zaal, P. A., de Koter, A., Marlborough, J. M., Millar, C. E., Trams, N., Morris, P. W., & de Graauw, T., 2000. *A&A* **355**, 187.

Kastner, J. H. & Mazzali, P. A., 1989. *A&A* **210**, 295.

Kwan, J. & Krolik, J. H., 1981. *ApJ* **250**, 478.

Marlborough, J. M., 1969. *ApJ* **156**, 135.

Millar, C. E. & Marlborough, J. M., 1998. *ApJ* **494**, 715. (MM).

Millar, C. E. & Marlborough, J. M., 1999a. *ApJ* **516**, 280. (MMa).

Millar, C. E. & Marlborough, J. M., 1999b. *ApJ* **516**, 276. (MMb).

Osterbrock, D. E., 1989. *Astrophysics of Gaseous Nebulae and Active Galactic Nuclei*. Mill Valley: University Science Books.

Poeckert, R. & Marlborough, J. M., 1978. *ApJ* **220**, 940. (PM).

Puls, J., Petrenz, P., & Owocki, S. P., 1999. In B. Wolf and A. W. Fullerton (Eds.), *IAU Colloq. 169, Variable and Non-spherical Stellar Winds in Luminous Hot Stars*. Germany. Springer-Verlag.

Quirrenbach, A., Bjorkman, K. S., Bjorkman, J. E., Hummel, C. A., Buscher, D. F., Armstrong, J. T., Mozurkewich, D., II, N. M. E., & Babler, B. L., 1997. *ApJ* **479**, 477.

Stee, P., de Araújo, F. X., Vakili, F., Mourard, D., Arnold, L., Bonneau, D., Morand, F., & Tallon-Bosc, I., 1995. *A&A* **300**, 219.

Stee, P., Vakili, F., Bonneau, D., & Mourard, D., 1998. *A&A* **332**, 268.

van Kerkwijk, M. H., Waters, L. B. F. M., & Marlborough, J. M., 1995. *A&A* **300**, 259.

Vogt, S. S. & Penrod, G. D., 1983. *ApJ* **275**, 661.

Wood, K., Bjorkman, K. S., & Bjorkman, J. E., 1997. *ApJ* **477**, 926.

Chapter 7

Conclusions

7.1 Theoretical Models

Theoretical models which describe the physical conditions in Be star envelopes are steadily improving due to both the increasing speed and capacity of computers and improvements in observational techniques which enable parameters used in model calculations to be determined with greater certainty. However, the mechanism(s) by which the disks are produced and maintained is still not presently known. A variety of models such as the wind compressed disk model (Bjorkman and Cassinelli 1993), non-radial pulsations (Vogt and Penrod 1983), and non-spherical, radiatively-driven wind models (Puls, Petrenz, and Owocki 1999) among others have been proposed to attempt to explain the formation and maintenance of these disks. None has been completely successful.

Any reduction in the number of free parameters of a particular model helps to further constrain the model and hopefully find one that is satisfactory. My technique, which satisfies the equation of energy conservation, enables the thermal structure of the envelope to be calculated based on equating the rates of energy gain and loss. In order to predict spectral lines one requires an accurate description of the internal structure of the envelope including number densities and ionization fractions. Improvements in determining these quantities enable more precise calculation of optical depths, locations in the envelope where various lines are formed and better estimates of the rotational velocity of the disk from the Doppler broadening of these lines.

7.2 Envelope Temperature Distributions

Given a density and velocity distribution, both a self-consistent ionization-excitation equilibrium and electron temperature can be obtained. The atomic level populations are obtained from the solution of the statistical equilibrium equations based on an initial assumed temperature at each prescribed grid point. Then the rates of energy gain and loss are evaluated based on the level populations. The temperature is adjusted at each location depending on the value of the ratio of energy gain to loss. Then the level populations are re-calculated via the statistical equilibrium equations. This process is repeated until the ratio of energy gain to loss is equal to 1 within some prescribed value.

The processes I have included in the rates of energy gain and loss are photoionization, radiative recombination, collisional transitions between bound level, free-free absorption and free-free emission. Generally, for the Be star envelopes investigated to date, the most important processes in terms of relative magnitude are photoionization and radiative recombination. The free-free terms were not generally very important but were included for completeness. If, in the future, processes other than those listed above were determined to be important, these could also be included in the energy rate equations and new temperature distributions determined. My method will improve a model's diagnostic capabilities for calculating the physical conditions in circumstellar disks. Self-consistent temperatures are critical to determining the correct thermal structure and ionization balance within the wind.

My investigations have focussed on γ Cas, an early-type Be star, and 1 Del, a late-type Be star, since both of these stars have been well studied and cover the range of typical Be stars.

7.2.1 Results

The temperature averages given in Table 7.1 are based on self-consistent model temperature distributions calculated using the PM model density distribution (Poeckert and

Table 7.1: A comparison of envelope temperatures with and without diffuse radiation for both 1 Del and γ Cas

	global average [K]	global average including diffuse radiation [K]	density weighted average [K]	density weighted average including diffuse radiation [K]
γ Cas	12000±4000	14000±3000	10700±90	14500±80
1 Del	5800±1000	6900±1700	5900±40	7200±50

Marlborough 1978). Columns 2 and 3 are simple global averages of the temperature at the grid points considered and columns 4 and 5 are density weighted averages calculated by weighting the temperature at a position by the density there. The density weighted averages are dominated by regions both near the star and the equatorial plane. The model parameters with and without diffuse radiation are identical in order to evaluate the change in temperature produced by this radiation. These average temperatures are considerably lower than the isothermal temperatures of 20000 K and 10000 K, assumed by PM and Marlborough and Cowley (1974), for γ Cas and 1 Del, respectively. The diffuse radiation produced within the envelope is included using the on-the-spot approximation (Osterbrock 1974) which removes the necessity of solving the transfer equation about 4π steradians. Table 7.1 clearly demonstrates that the inclusion of the diffuse radiation field increases the average envelope temperature. The diffuse radiation field provides additional heating due to the increase in photoionization from level n = 1. This increases the ionization fraction which subsequently increases the number of recombinations, with the result that the emission lines also increase in strength. As a result, in order to match predicted lines with observed lines, the assumed value of ρ_2, which is used to calculate the density distribution along the equatorial plane using the equation of continuity, must be reduced by approximately a factor of 3. This illustrates the fact that all processes which affect the thermal structure must be included if a reasonable range of model parameters is to be ascertained.

An independent temperature calculation for the envelope of γ Cas by Hony et al. (2000) based on the observed size of the Humphreys (6-∞) bound-free jump at 3.4 μm was determined to be 9500 $\pm$ 1000 K. The emission in the Humphreys continuum is expected to originate from the denser regions of the envelope and by comparison with Table 7.1 column 4, it is clear this independent temperature calculation agrees very well with my density weighted temperature which matches the relative emission of the Hα line. It is appropriate to compare column (4) of Table 7.1 with this temperature calculation because the temperatures in columns (5) and (6) which include the diffuse field, as discussed earlier, greatly over-estimate the relative strength of the Hα line. Furthermore, the on-the-spot approximation represents an upper limit to the temperature.

I have also applied this temperature analysis to a model originally developed by Waters (1986) and I investigated a range of Be stars using the same parameters as Waters et al. (1987) in order to test the appropriateness of the temperatures assumed. The numerical value of the ratio of the rate of energy gain to rate of energy loss provides a measure of how good or otherwise the assumed temperatures are. In each case the assumed temperatures were too high by a factor of 2 to 3. Then, self-consistent temperature distributions were calculated using the same envelope parameters as Waters. The results are displayed in Table 7.2. Given the importance of the diffuse field to the PM model temperature calculations, it would be interesting to add the diffuse field to this model also.

In a recent parameter study of the disk model for the Be star φ Per, the line shapes and ratios of line strengths were found to be strongly dependent on the temperature structure of the envelope (Marlborough et al. 1997). Therefore, a self-consistent temperature distribution is an essential step to determine the physical parameters that describe conditions in the envelopes of Be stars.

I have also computed hydrogen line fluxes emitted in the important Hα, Pα, and Brα transitions by the circumstellar envelopes of early-type and late-type Be stars. These line fluxes are based on models with self-consistent envelope temperatures which balance local

Table 7.2: Assumed and calculated disk model temperatures

Name	Spectral Type	Assumed Wind Temperature [K]	Calculated Average Temperature [K] of Ratios ($\pm 1\sigma$)
γ Cas	B0IVe	25000	13000±1000
δ Cen	B2IVne	16000	5600±2500
ζ Per	B5Ve	12000	4200±1500
β CMi	B8Ve	10000	4400±1200

energy loss and gain and which, individually, match the relative Hα line profiles of γ Cas and 1 Del. Using these models as typical of Be stars of their respective spectral types, I find that I can also successfully match the absolute Hα line fluxes of Ashok et al. (1984) for both early and late type Be Stars. My results are in disagreement with the suggestion of Apparao and Tarafdar (1987) that an additional source of UV photoionizing radiation is required to explain the absolute Hα line fluxes from late-type Be stars. The observed Hα fluxes are consistent with the underlying stellar photosphere as the only source of energy input into the circumstellar disks.

Comparing my results in Table 6.2 with these observations, I find no clear case for an additional source of ionizing radiation in order to produce the observed Hα emission for our particular choice of model parameters for either γ Cas or 1 Del. The discrepancies between Apparao's work and my calculations are due mainly to my realistic 2D geometry, and the inclusion of collisional excitation and optical depths in Hα. In addition, I also concluded from this analysis that case B recombination is inappropriate for the calculation of hydrogen line fluxes from Be envelopes, and this issue is also discussed by Hony et al. (2000).

7.3 Future Work

Metals, such as iron, could be included in my models. Since the abundance of heavy elements is quite low, it is not expected that metals will have a significant effect on the thermal structure, for example, via line cooling. However, a correct self-consistent temperature distribution will enable the various ionization zones for particular metals to be accurately determined. Thus, the region of the envelope where they are formed could easily be determined. In addition, the rotational broadening of these particular lines will enable the rotational velocity distribution as a function of distance from the star to be better determined.

It would be interesting to modify the models so that B[e] stars could be investigated. B[e] stars are a diverse group of stars ranging from main sequence stars, evolved proto-planetary nebulae and massive hot supergiants (Zickgraf 2000). B[e] stars are characterized by an absorption line spectra similar to normal B stars and in addition, H I, He I, Fe II, and Mg II emission lines, [Fe II] and [S II] forbidden emission lines, linear polarization but generally no variability and outbursts are observed (Marlborough 2000). These stars are also observed to have an infrared excess due to hot dust. A study of these stars may be interesting since both Be and B[e] stars are characterized by non-spherical winds. It thought that a low luminosity sub-class of the B[e] stars may be somehow related to the Be stars, perhaps they are an extension of the Be phenomenon into other regions of the HR diagram (Marlborough 2000).

I have begun a preliminary investigation of the relative magnitudes of the gas dynamical terms in the Be star envelopes. It will be valuable to have a complete set of values for these dynamical terms throughout the envelope to evaluate the stability properties of the gas with various temperature and density distributions. It would be interesting to see if these disks could develop convective regions.

7.4 Summary

The development of my technique to determine self-consistently the temperature distribution in Be star envelopes is an important and necessary step to

reveal the thermal structure in Be star disks which will ultimately lead to improvements in models. Physical characterization of the disk is crucial to understanding the processes by which such disks are formed and maintained.

Bibliography

Apparao, K. M. V. & Tarafdar, S. P., 1987. *ApJ* **322**, 976.

Ashok, N. M., Bhatt, H. C., Kulkarni, P. V., & Joshi, S. C., 1984. *MNRAS* **211**, 471.

Bjorkman, J. E. & Cassinelli, J. P., 1993. *ApJ* **409**, 429.

Hony, S., Waters, L. B. F. M., Zaal, P. A., de Koter, A., Marlborough, J. M., Millar, C. E., Trams, N., Morris, P. W., & de Graauw, T., 2000. *A&A* **355**, 187.

Marlborough, J. M., 2000. Summary and future directions. In M. A. Smith, H. F. Henrichs, and J. Fabregat (Eds.), *IAU Colloq. 175, The Be Phenomenon in Early-Type Stars*.

Marlborough, J. M. & Cowley, A. P., 1974. *ApJ* **187**, 99. (MC).

Marlborough, J. M., Zijlstra, J. W., & Waters, L. B. F. M., 1997. *A&A* **321**, 867.

Osterbrock, D. E., 1974. *Astrophysics of Gaseous Nebulae*. U.S.A.: W.H. Freeman and Company.

Poeckert, R. & Marlborough, J. M., 1978. *ApJ* **220**, 940. (PM).

Puls, J., Petrenz, P., & Owocki, S. P., 1999. In B. Wolf and A. W. Fullerton (Eds.), *IAU Colloq. 169, Variable and Non-spherical Stellar Winds in Luminous Hot Stars*. Germany, Springer-Verlag.

Vogt, S. S. & Penrod, G. D., 1983. *ApJ* **275**, 661.

Waters, L. B. F. M., 1986. *A&A* **162**, 121.

Waters, L. B. F. M., Coté, J., & Lamers, H. J. G. L. M., 1987. *A&A* **185**, 206.

Zickgraf, F., 2000. The connection with B[e] stars. In M. A. Smith, H. F. Henrichs, and J. Fabregat (Eds.), *IAU Colloq. 175, The Be Phenomenon in Early-Type Stars*.